The SPD (Spin Physics Detector) experiment at NICA

Alexander Korzenev, on behalf of the SPD Collaboration

NPCS seminar, Minsk
June 19-23, 2023

~300 participants from 32 institutes from 15 countries

SPD project at NICA (JINR, Dubna)

- SPD (Spin Physics Detector) is a universal facility with the primary goal to study *unpolarized and polarized gluon content of proton and deuteron*
- SPD project was approved by PAC JINR and had its first proto-collaboration meeting in June 2019
- Conceptual Design Report (CDR) was released in January 2021, [arXiv:2102.00442]
- Official birthday of the SPD collaboration in June 2021
- Technical Design Report (TDR) v1 of SPD was released in January 2023
- Beginning of datataking (1-st stage) by 2028

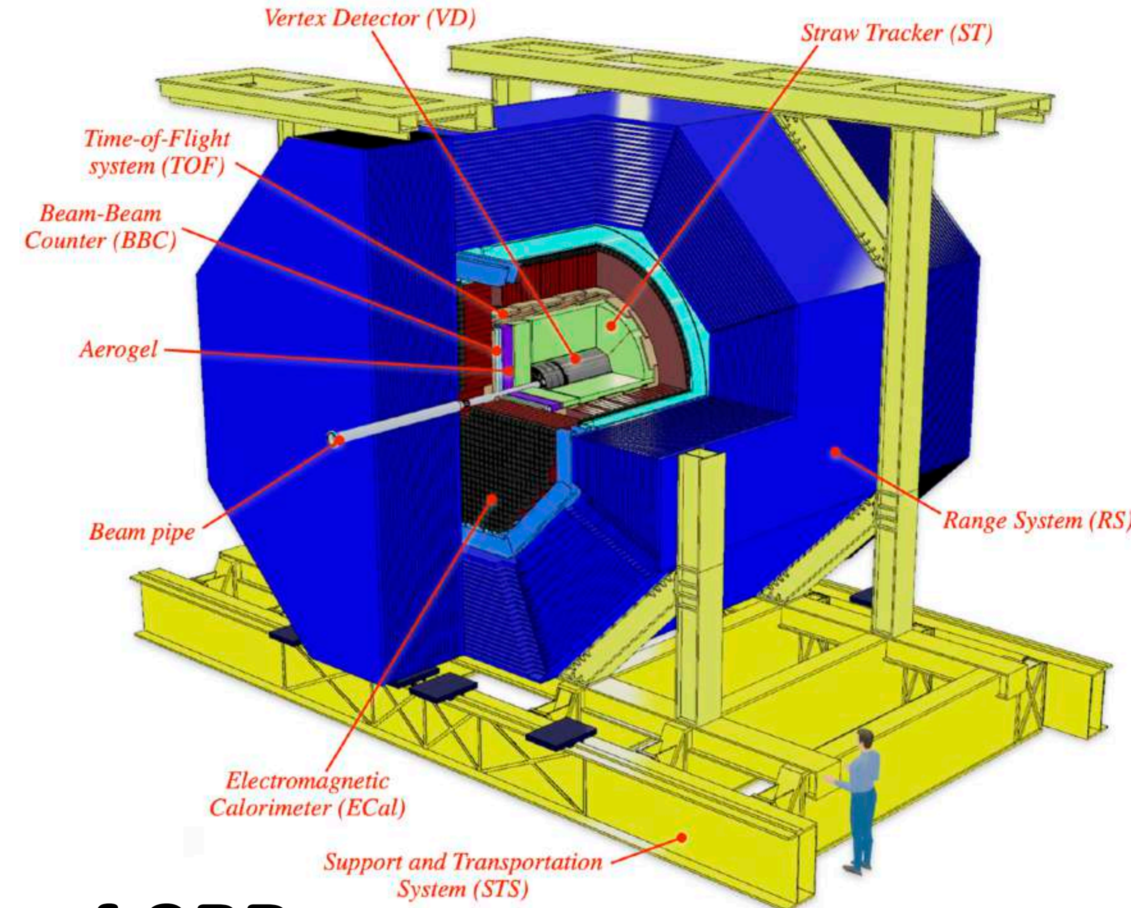

Physics program of SPD

- A.Arbuzov et al, *On the physics potential to study the gluon content of proton and deuteron at NICA SPD*, Prog.Part.Nucl.Phys. 119 (2021) 103858 [arXiv:2011.15005]
  - Probe gluon distributions in production of charmonia, open charm and prompt photons
- V.Abramov et al, *Possible studies at the first stage of the NICA collider operation with polarized and unpolarized proton and deuteron beams*, Phys.Part.Nucl. 52 (2021) 6 [arXiv:2102.08477]
  - Spin effects in elastic scattering and hyperon production, study of multiquark correlation, dibaryon resonances, exclusive reactions, open charm and charmonia near threshold, …

Outline

- NICA accelerator complex in JINR Dubna
  - Injectors, Booster, Nuclotron, Collider, Experiments
- Detector subsystems of SPD
  - Magnet, RS, ECal, TOF, FARICH, ST, ITS, BBC, ZDC
- Physics program of the SPD experiment
  - Transverse momentum-dependent (TMD) distributions
  - Quark and gluon Sivers effects in proton
  - MC estimates for SSA statistical uncertainties
- Summary

Accelerator complex NICA in JINR

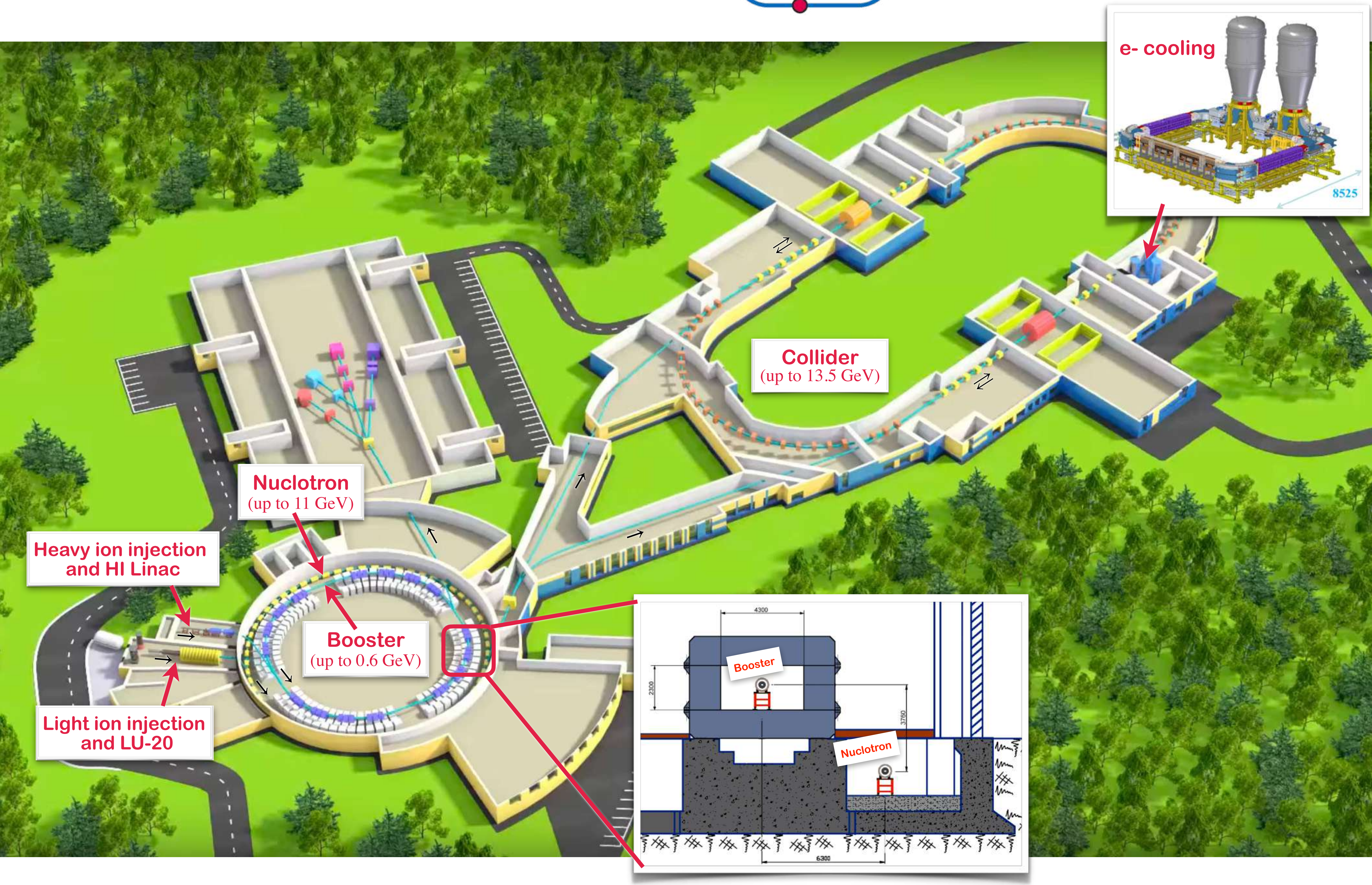

Experiments at NICA in JINR

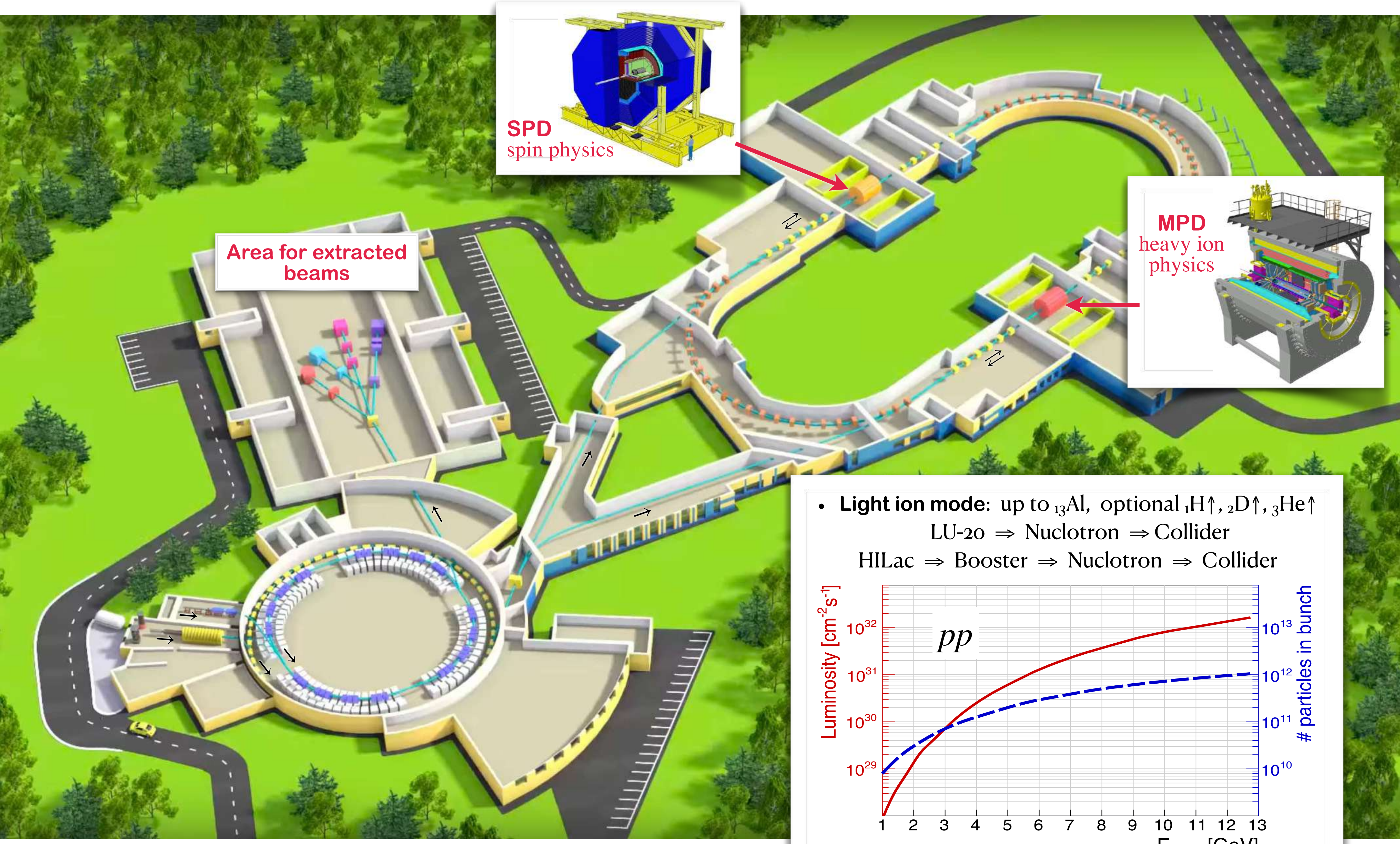

- **Light ion mode:** up to $_{13}$Al, optional $_1$H↑, $_2$D↑, $_3$He↑

LU-20 ⇒ Nuclotron ⇒ Collider

HILac ⇒ Booster ⇒ Nuclotron ⇒ Collider

MPD experimental hall

(detector is designed for high particle multiplicity and low trigger rates)

- The year 2023 will be dedicated to testing the magnet
- All detectors will be mounted in 2024
- The first run in January 2025

SPD experimental hall

(detector is designed for low particle multiplicity and high trigger rates)

- The SPD hall is currently used for storing concrete blocks of biological protection and collider elements
- The first run is planned for the end of this decade

SPD compared to other spin experiments

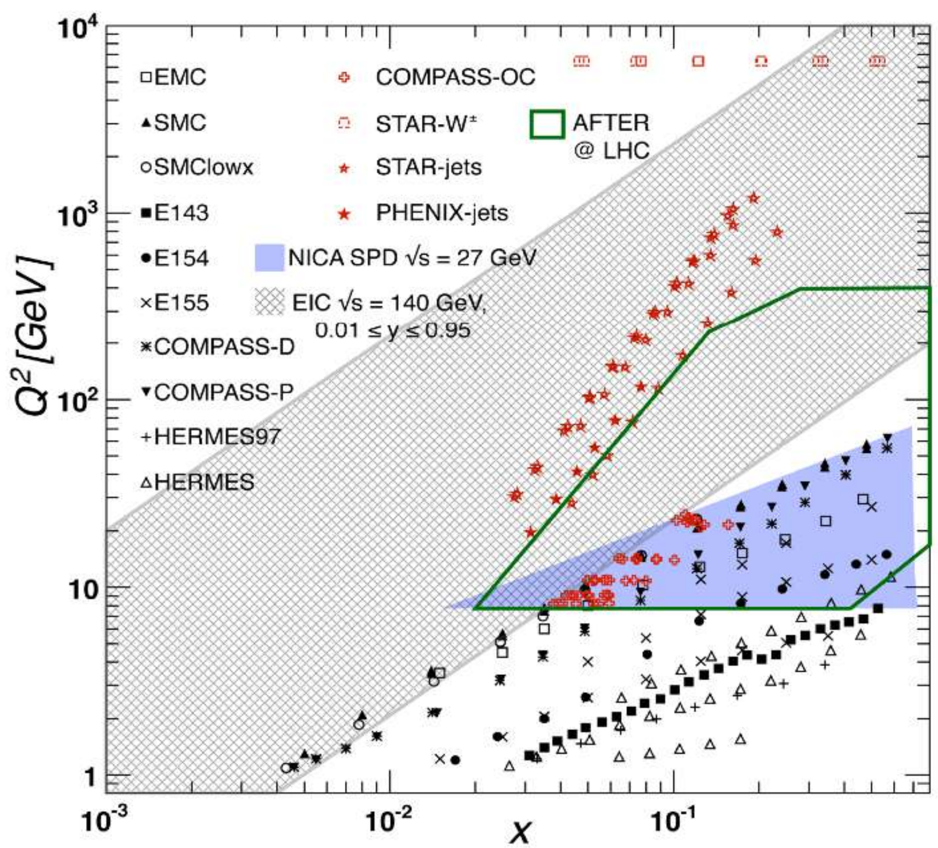

Main present and future gluon-spin-physics experiments

Experimental facility	SPD @NICA	RHIC	EIC	AFTER @LHC	LHCspin
Scientific center	JINR	BNL	BNL	CERN	CERN
Operation mode	collider	collider	collider	fixed target	fixed target
Colliding particles & polarization	$p^\uparrow$-$p^\uparrow$ $d^\uparrow$-$d^\uparrow$ $p^\uparrow$-d, p-$d^\uparrow$	$p^\uparrow$-$p^\uparrow$	$e^\uparrow$-$p^\uparrow$, $d^\uparrow$,^{3}He$^\uparrow$	p-$p^\uparrow$,$d^\uparrow$	p-$p^\uparrow$
Center-of-mass energy $\sqrt{s_{NN}}$, GeV	≤27 (p-p) ≤13.5 (d-d) ≤19 (p-d)	63, 200, 500	20-140 (ep)	115	115
Max. luminosity, 10^{32} cm^{-2} s^{-1}	~1 (p-p) ~0.1 (d-d)	2	1000	up to ~10 (p-p)	4.7
Physics run	>2025	running	>2030	>2025	>2025

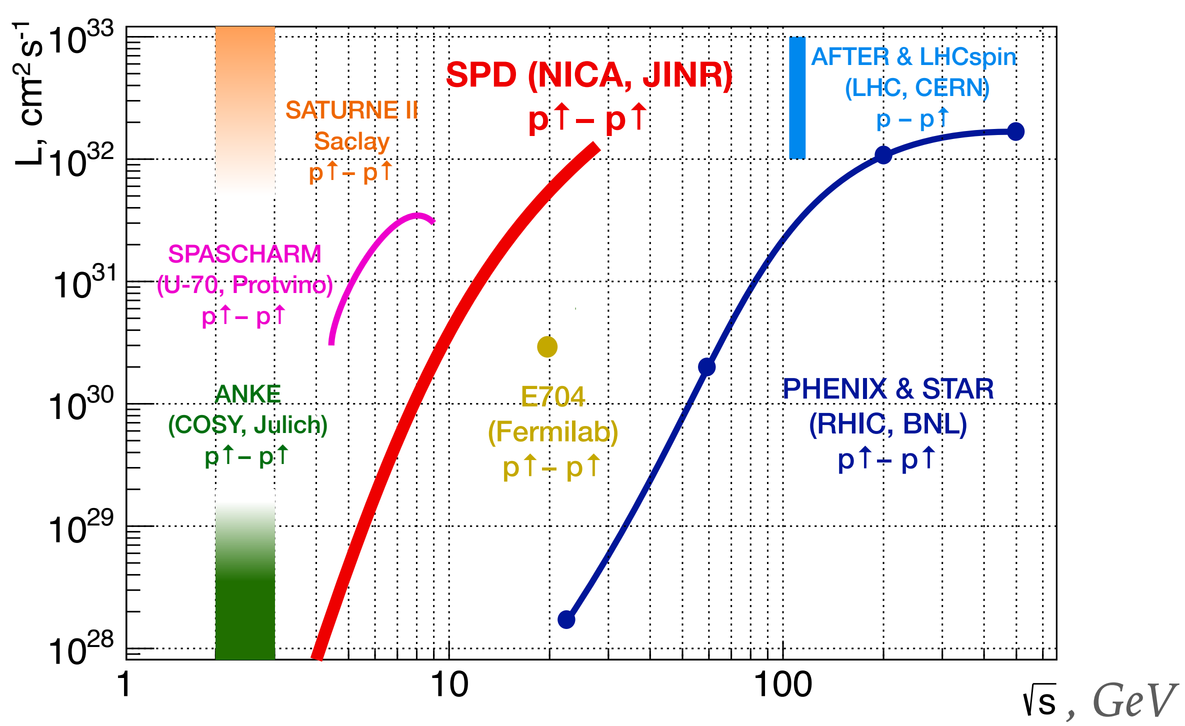

- Access to intermediate and high values of x
- Low energy but collider experiment (compared to fixed target). Nearly 4π coverage
- Two injector complexes available ⇒ mixed combinations p↑-d and p-d↑ are possible

Schematic view of the SPD setup

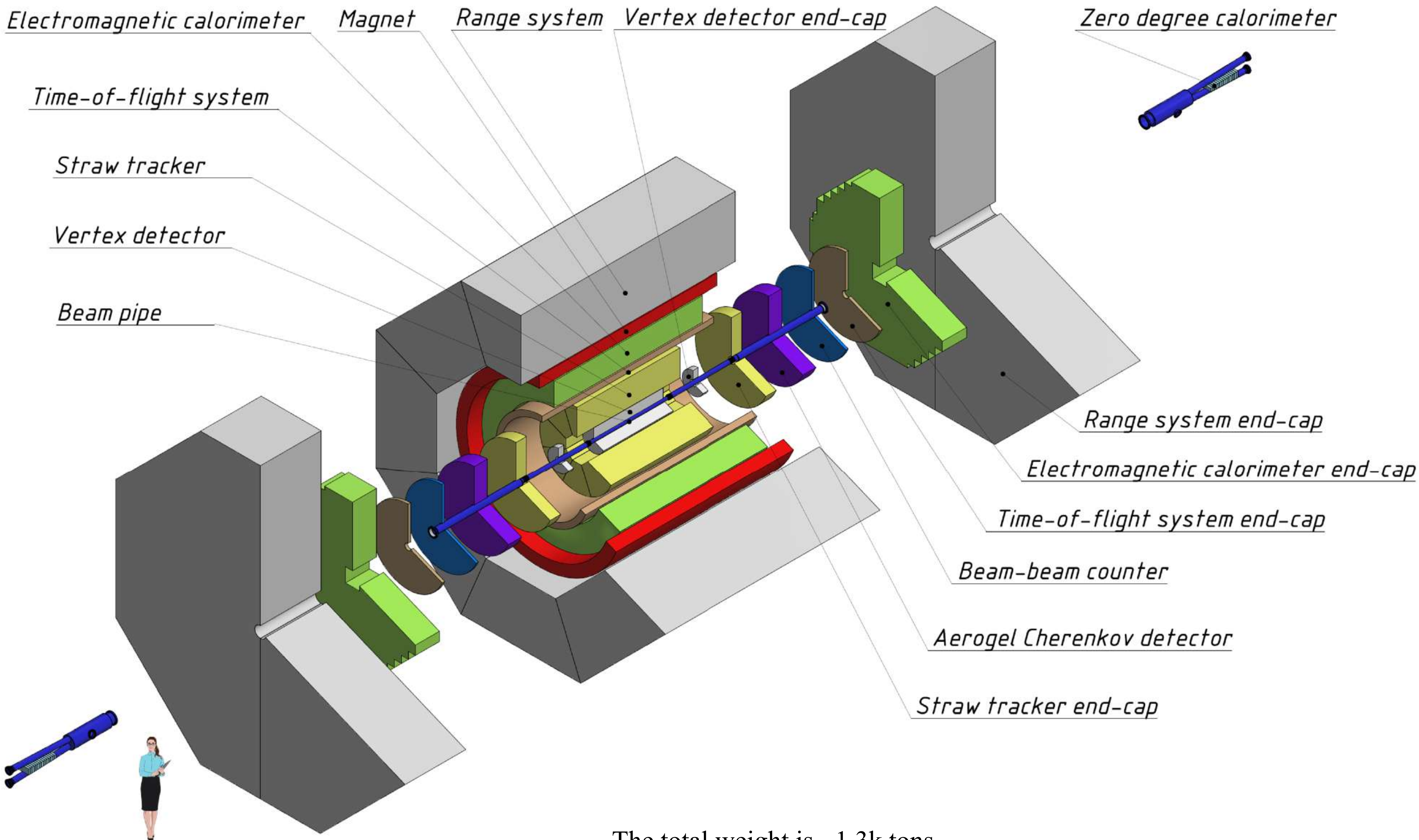

The total weight is ~1.3k tons

Superconductive solenoid magnet

Control Dewar
The volume of the Dewar tank is enough to cool the magnet offline for about a day without an influx of helium from the outside

Steel cryostat
Outer diameter 4.01 m
Inner diameter 3.47 m
Thickness 27 cm
Length 4.2 m
Weight 22 tons

Cooling He pipe welded to the support cylinder

Thermal shield cooled by gaseous He

Linear guides used for positioning an electro-magnetic calorimeter

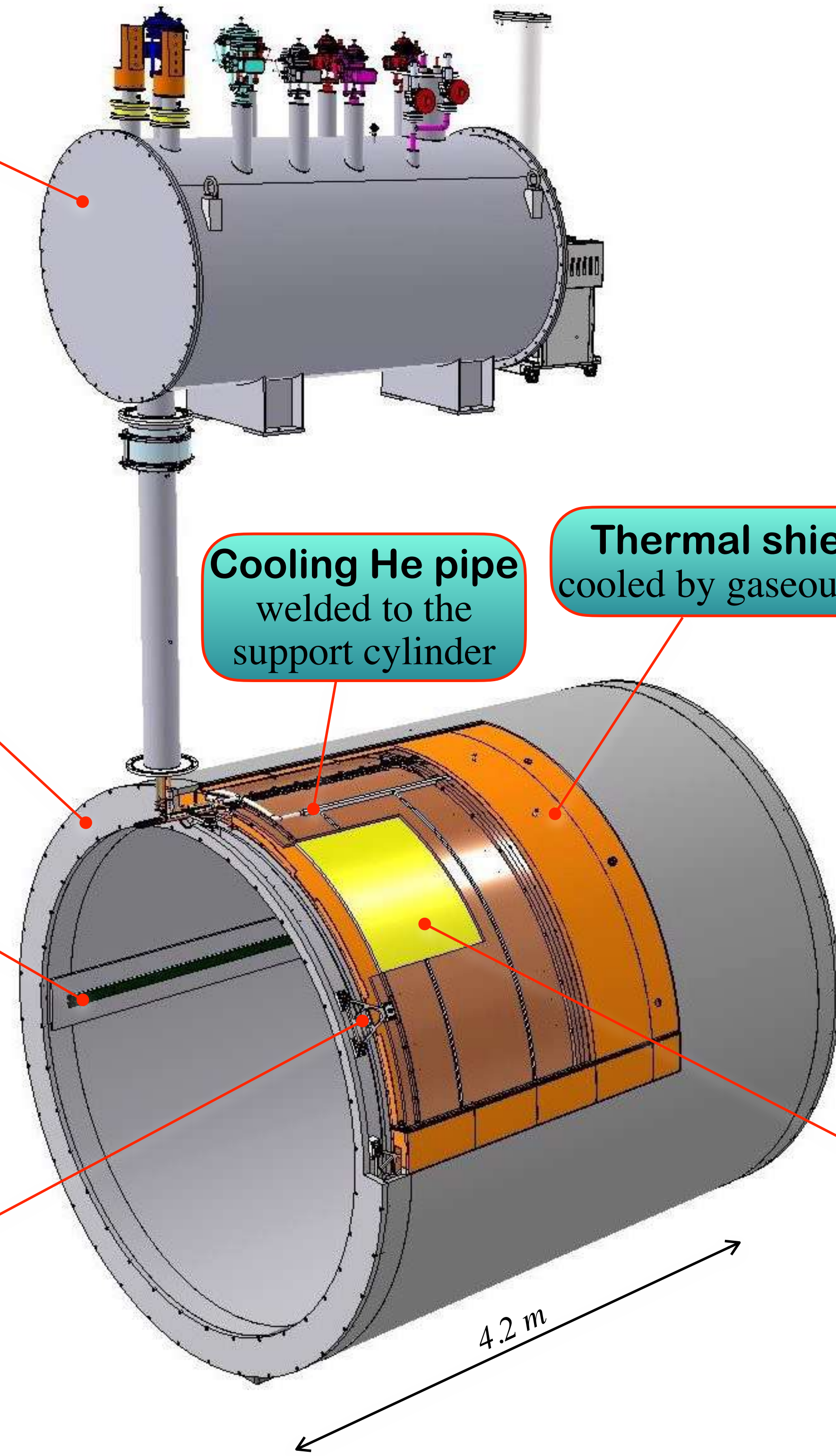

Triangular **supports** are used to suspend the “cold mass”.

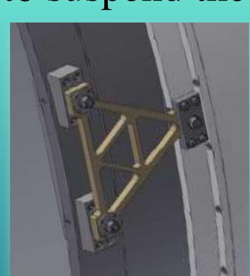

12 pieces on each side.

Made of fiberglass.

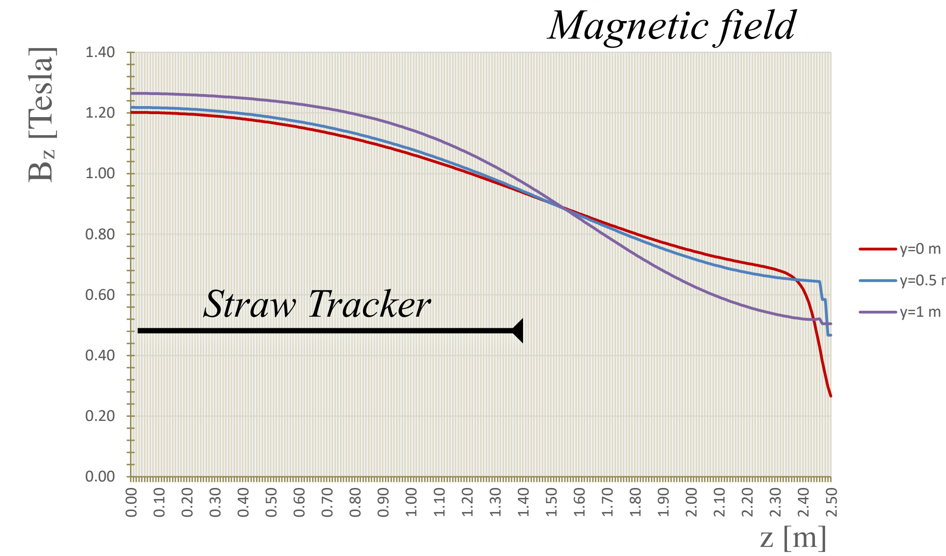

- 1.1 Tesla field with ±9% uniformity within ±1.4 m distance from center (tracking det.)
- Solenoid consists of 3 coils with 750 turns in total (two layer edge-wise winding)
  - central coil with 2×75=150 turns
  - 2 side coils with 2×150=300 turns
- The use of the *thermosyphon method* for cooling the superconducting coils (natural convection of two-phase helium at 4.5K)
- It will be constructed in BINP Novosibirsk

Rutherford-type cable made of 8-strands NbTi/Cu superconductor. The cable will be encased in an aluminum stabilizer using a co-extrusion process that provides a good bond between aluminum and superconductor in order to ensure quench protection during operation.

Range System (RS)

- Purposes: μ identification, rough hadron calorimetry, iron return yoke of the magnet, mechanical support structure of the overall detector
- 20 layers of Fe (3-6 cm) interleaved with gaps for Mini Drift Tube (MDT) detectors
- The endcaps must withstand the ~100 tonne magnetic force
- Total mass ~10^3 tons, at least $4\lambda_I$
- The design will follow closely the one of PANDA
- MDT provide 2 coordinate readout (~100 kch)
  - Al extruded comb-like 8-cell profile with anode wires + external electrodes (strips) perpendicular to the wires

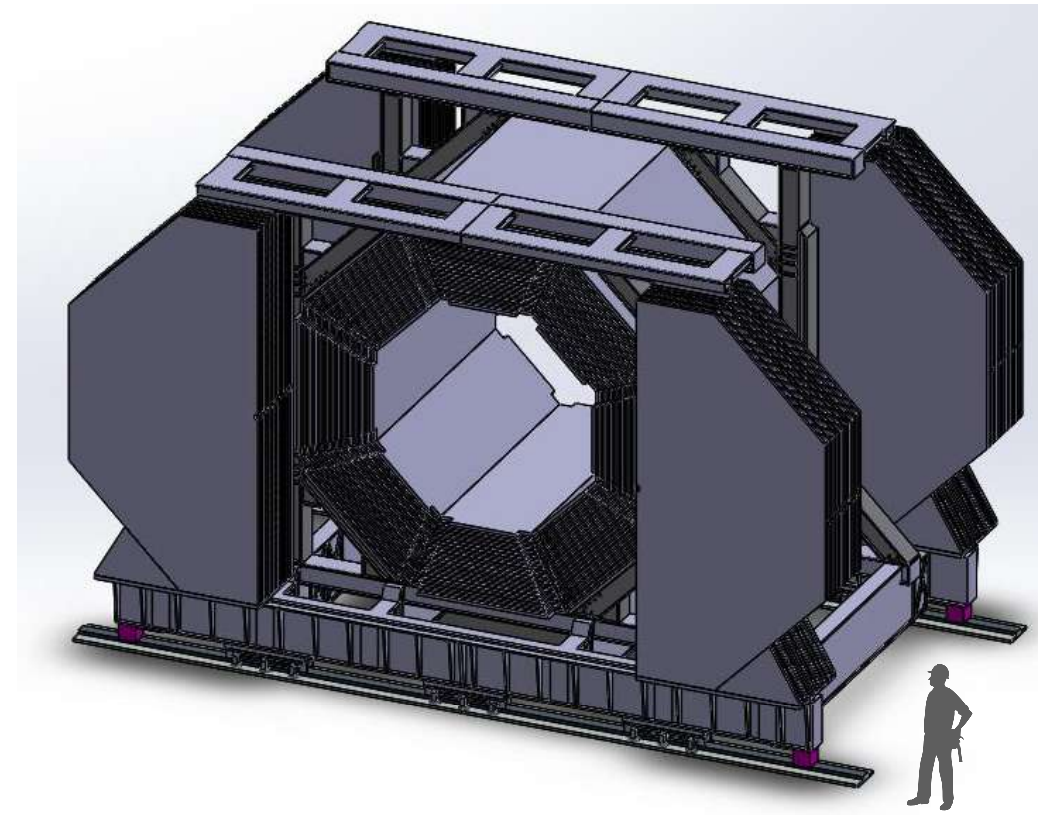

Results of beam tests of RS prototype (10 ton, 4k ch)

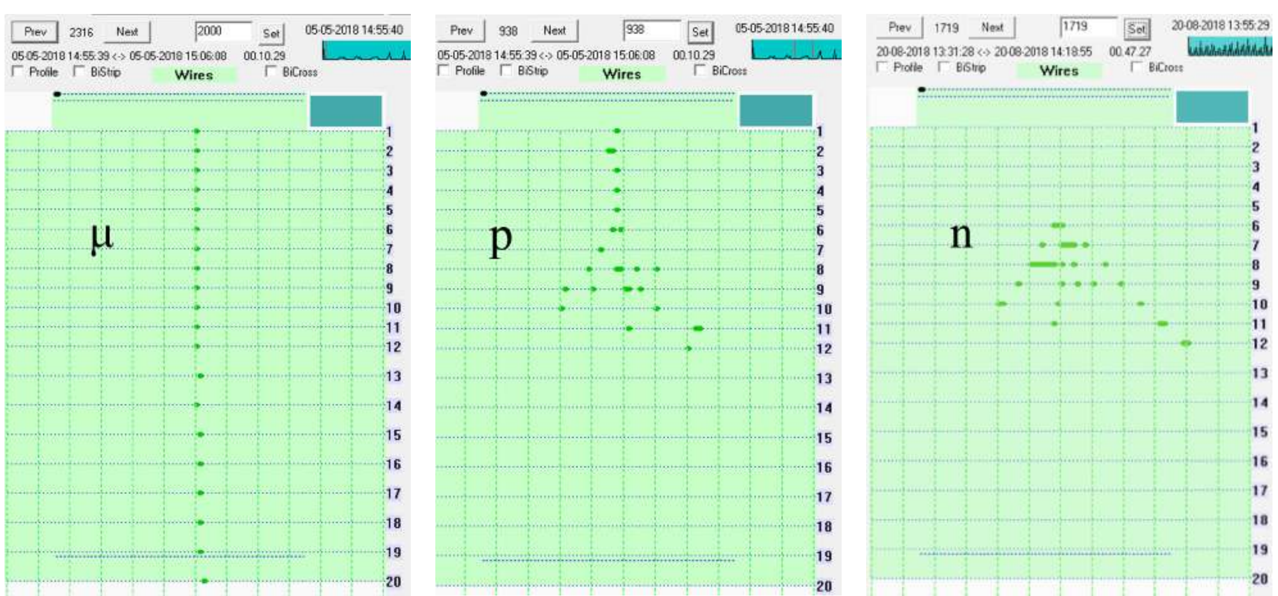

Mini Drift Tubes (MTD)

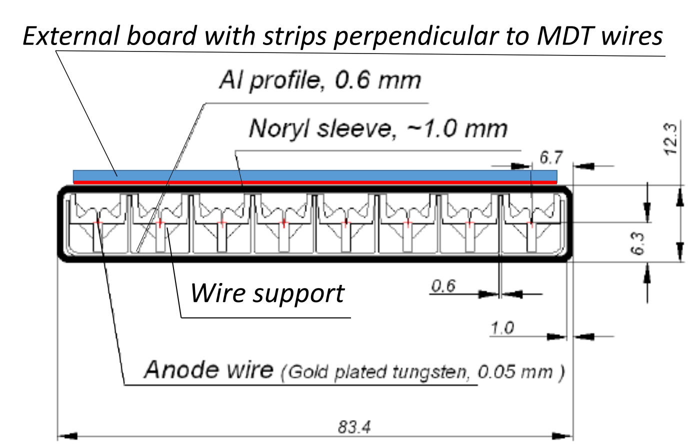

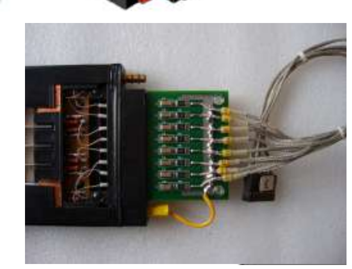

Electromagnetic Calorimeter (ECal)

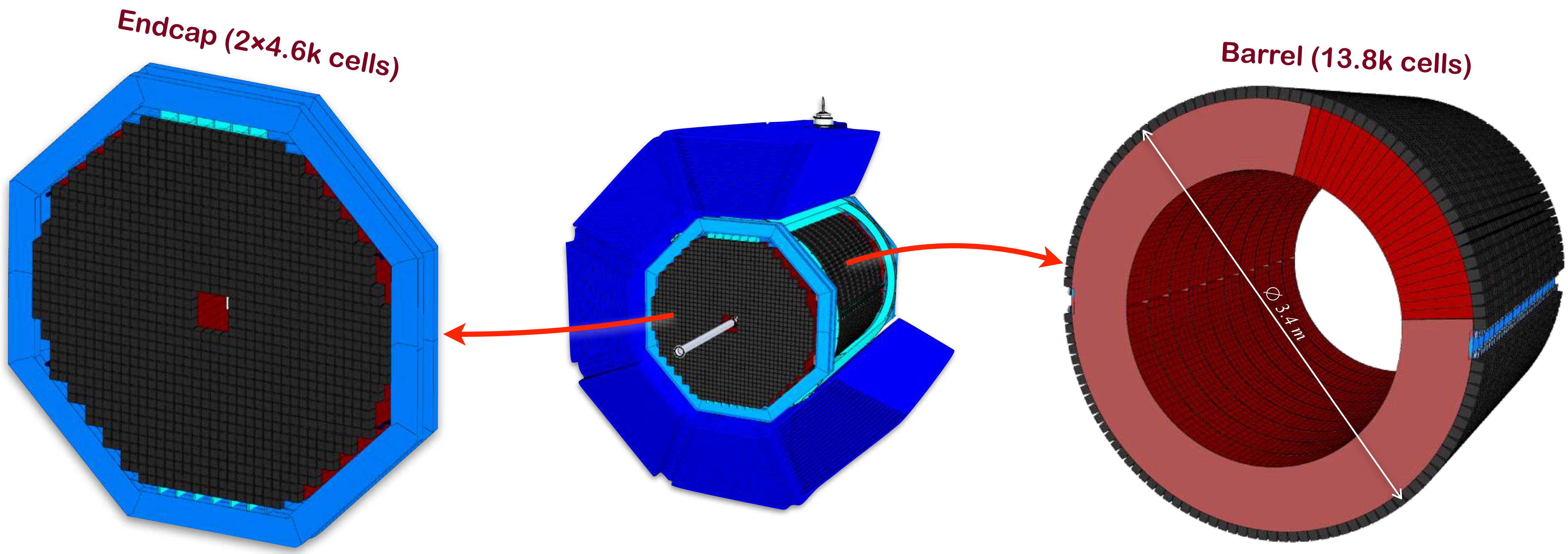

- Purpose: detection of prompt photons and photons from π^0, η and χ_c decays
- Identification of electrons and positrons
- Number of radiation lengths $18.6X_0$
- Total weight is 40t (barrel) + 28t (endcap) = 68t
- Total number of channels is ~23k
- Energy resolution is ~5% / $\sqrt{E}$
- Low energy threshold is ~50 MeV
- Time resolution is ~0.5 ns

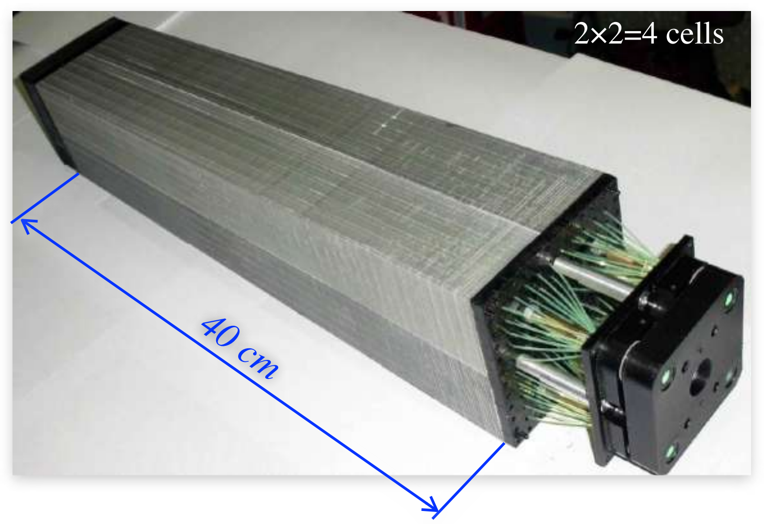

- 200 layers of lead (0.5 mm) and scintillator (1.5mm)
- 36 fibers of one cell transmit light to 6×6 mm^2 SiPM
- Moliere radius is ~2.4 cm

Time-of-flight (TOF) detector

Schematic view of self-sealed MRPC

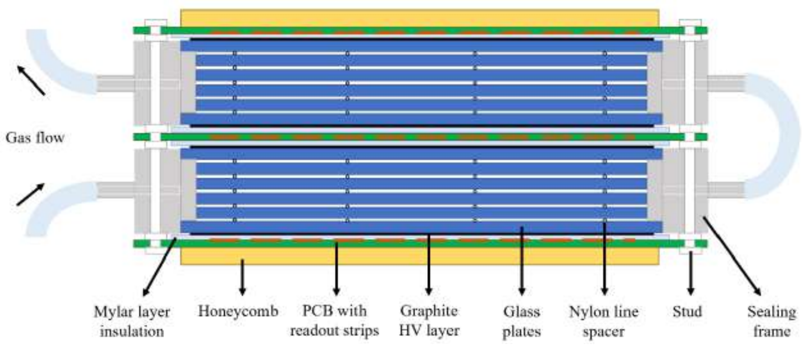

- Purpose: π/K/p discrimination for momenta ≲2 GeV, determination of t_0.
- Time resolution requirement <60 ps.
- Self-sealed Multigap Resistive Plate Chambers (MRPC) are the base option.
- Eco-friendly gas is under discussion HFO-1234ze ($C_3H_2F_4$) 4-th generation.
- Number of readout channels is ~12.2k

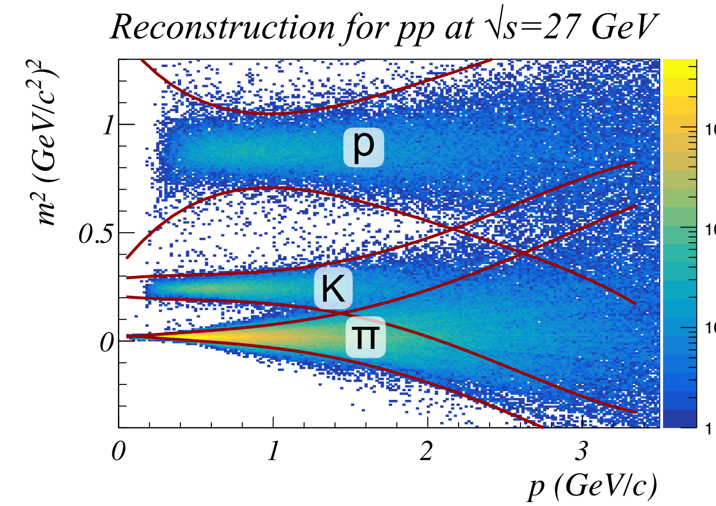

TOF Chambers for Barrel
(overlap in 2 dimensions)

16×9=144 MRPC

TOF Chamder
32 strips

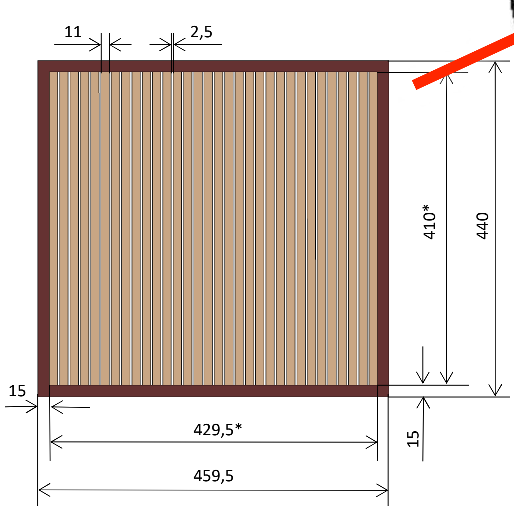

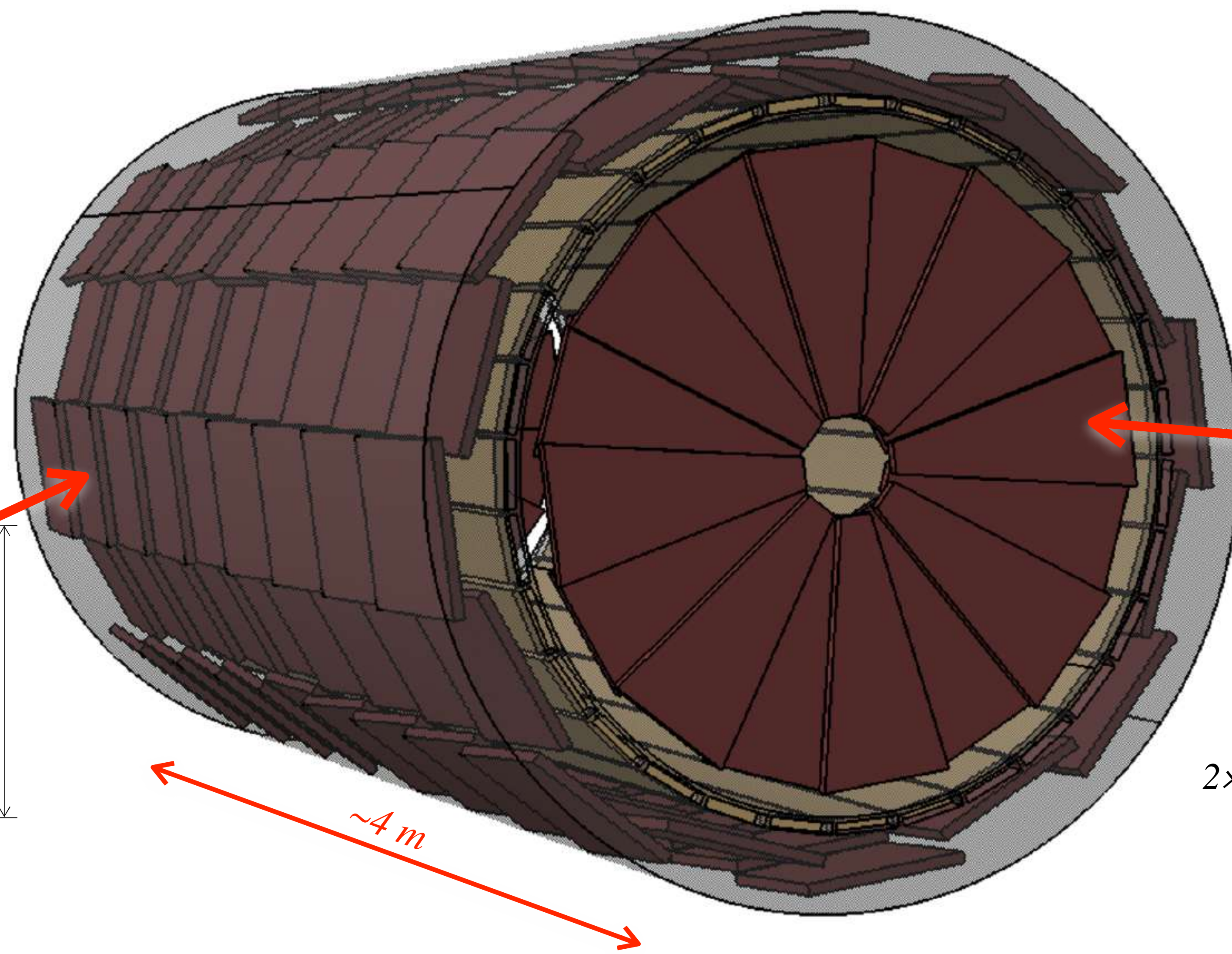

TOF Chambers for Endcap
48 strips

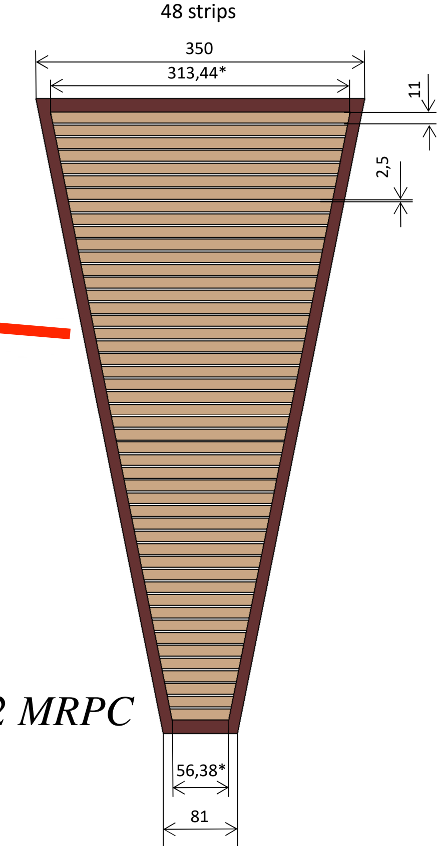

2×16=32 MRPC

Focusing Aerogel RICH (FARICH) detector

Principle of detector operation

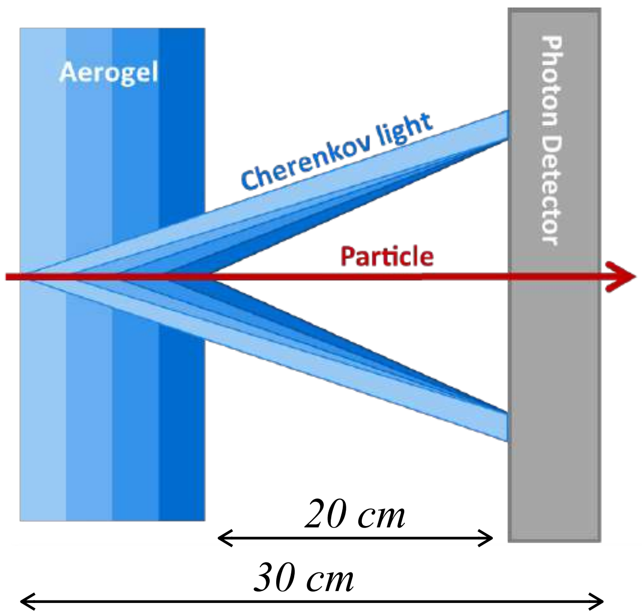

- Purpose: identification of high momentum particles ($p \gtrsim 1.5$ GeV) which cannot be discriminated by TOF
- Requirement: π/K separation at 6 GeV/c up to 3.5σ
- Disk-shaped detector in endcap with an area of 2 m^2
- Multilayer focusing aerogel radiator produced in BINP
- Development of Multi-anode MCP-PMT is ongoing in Russia (so far PMT of Hamamatsu, Photonis, Photek)
- The FARICH concept was published in 2005
- It was realized as a detector in Belle-II (KEK) in 2017

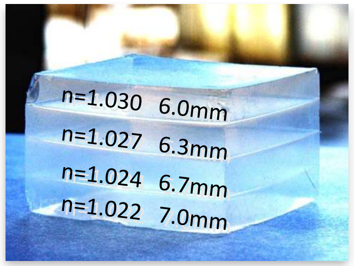

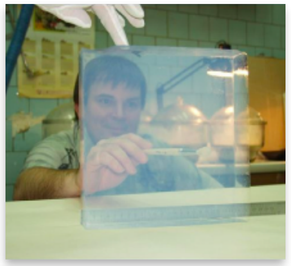

Accumulated *xy* distribution of hits

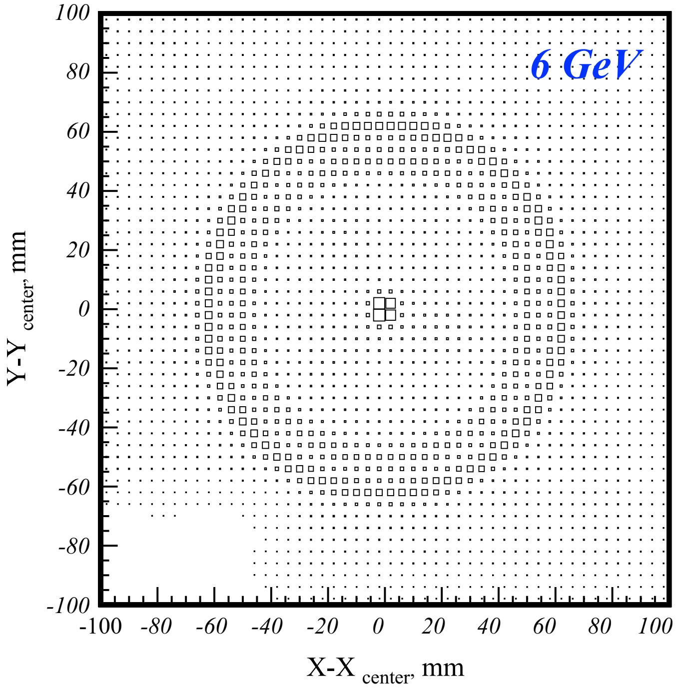

Ring radius distribution of γ

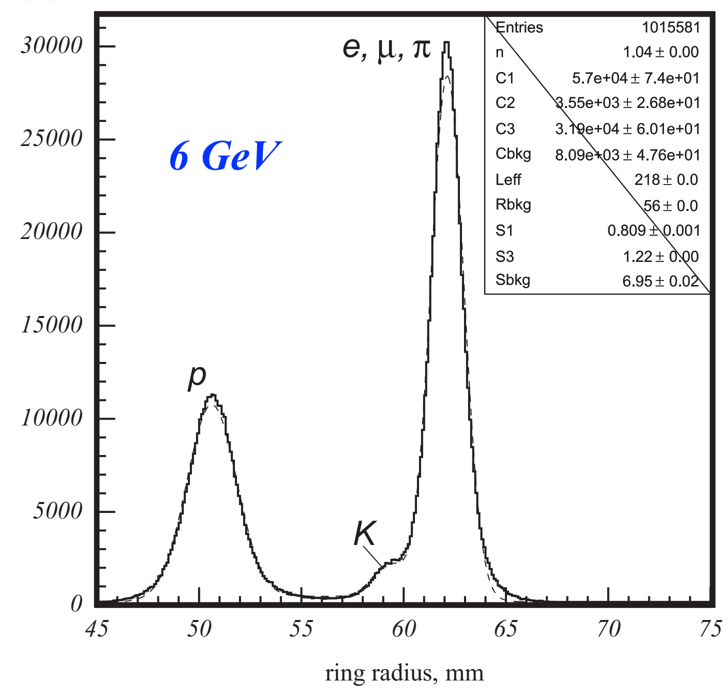

Ability to distinguish between π and K

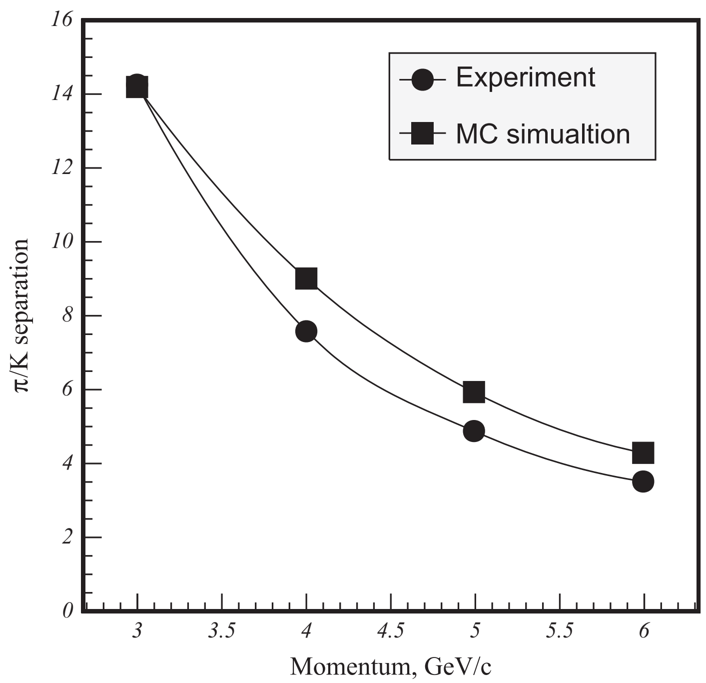

A.Barnyakov et al, NIMA732(2013)352

Barrel of Straw Tracker (ST)

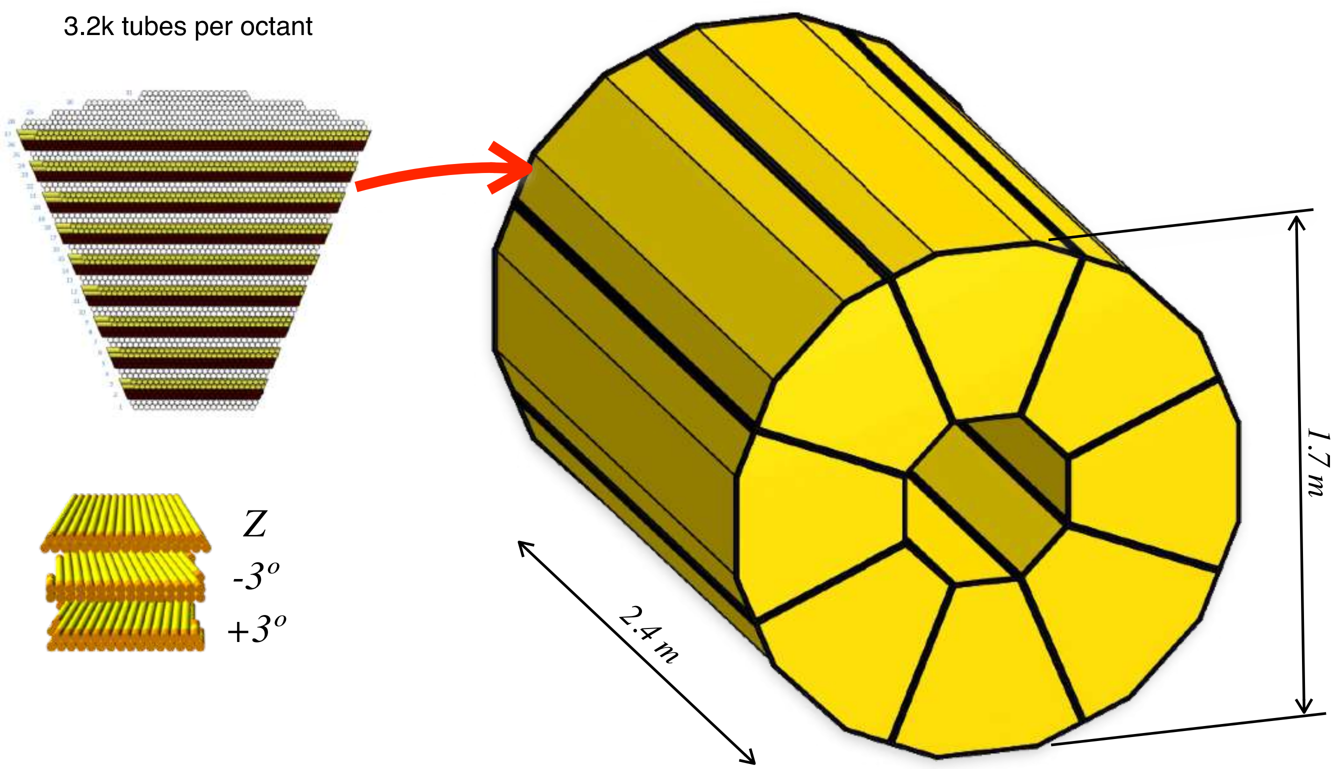

- Main tracker system of SPD
- Barrel is made of 8 modules with 30 double-layers oriented as *z,+3°,-3°*
- Maximum drift time of 120 ns for ∅=10mm straw
- Straw tubes are made of a PET foil that is ultrasonic welded to form a tube
- Spatial resolution of 150 μm
- Expected DAQ rate up to several hundred MHz/tube (electronics is limiting factor)
- Number of readout channels ~26k
- Extensive experience in straw production in JINR for several experiments: ATLAS, NA58, NA62, NA64; prototypes for: COZY-TOF, CREAM, SHiP, COMET, DUNE.

Energy loss in straw tubes

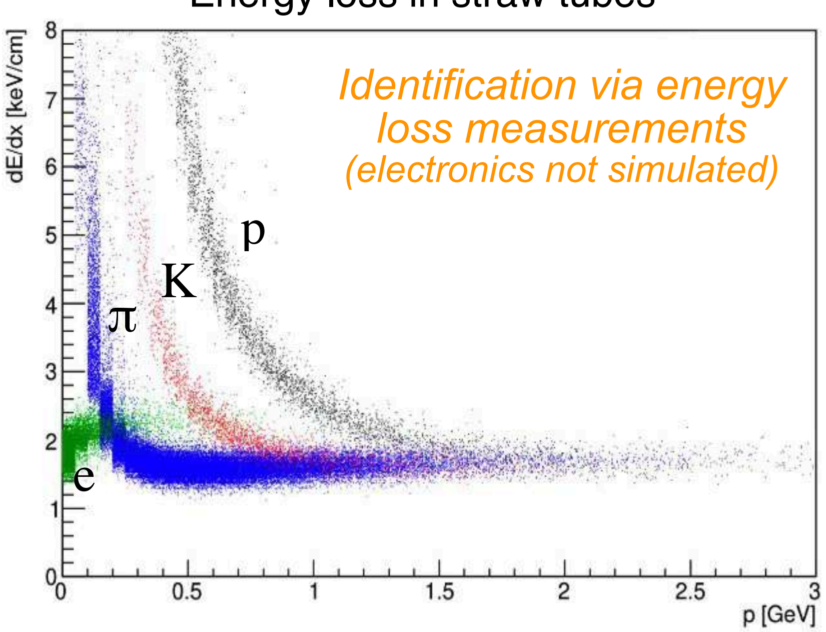

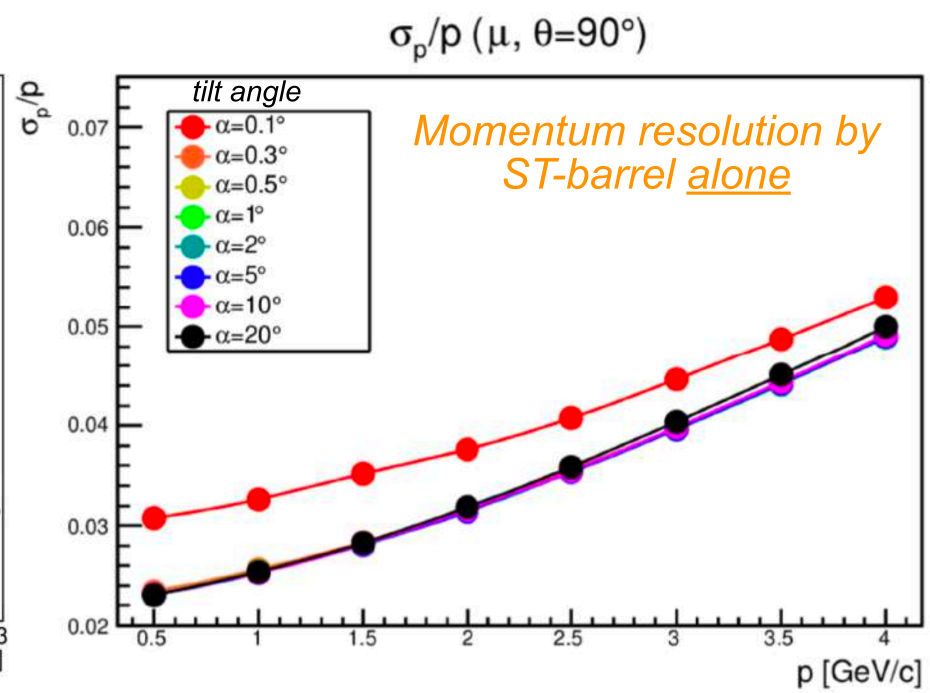

straw production for NA62 (~2010)

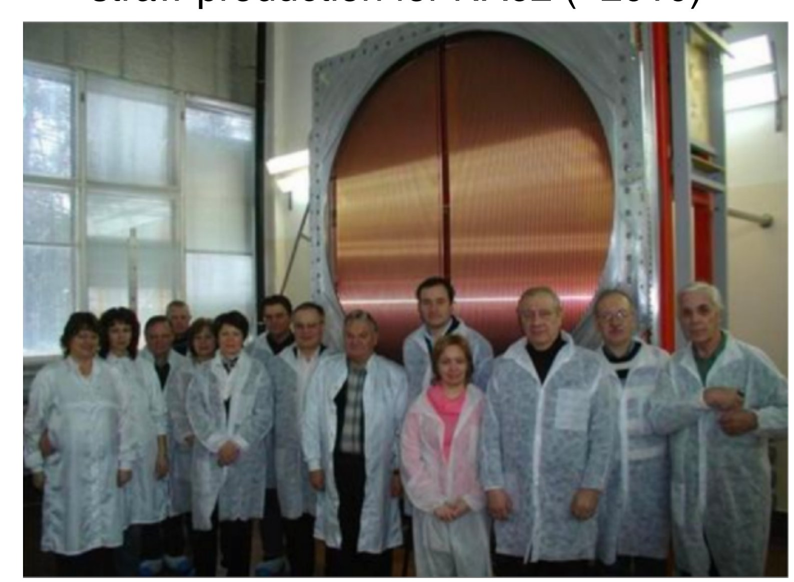

Endcap of Straw Tracker (ST)

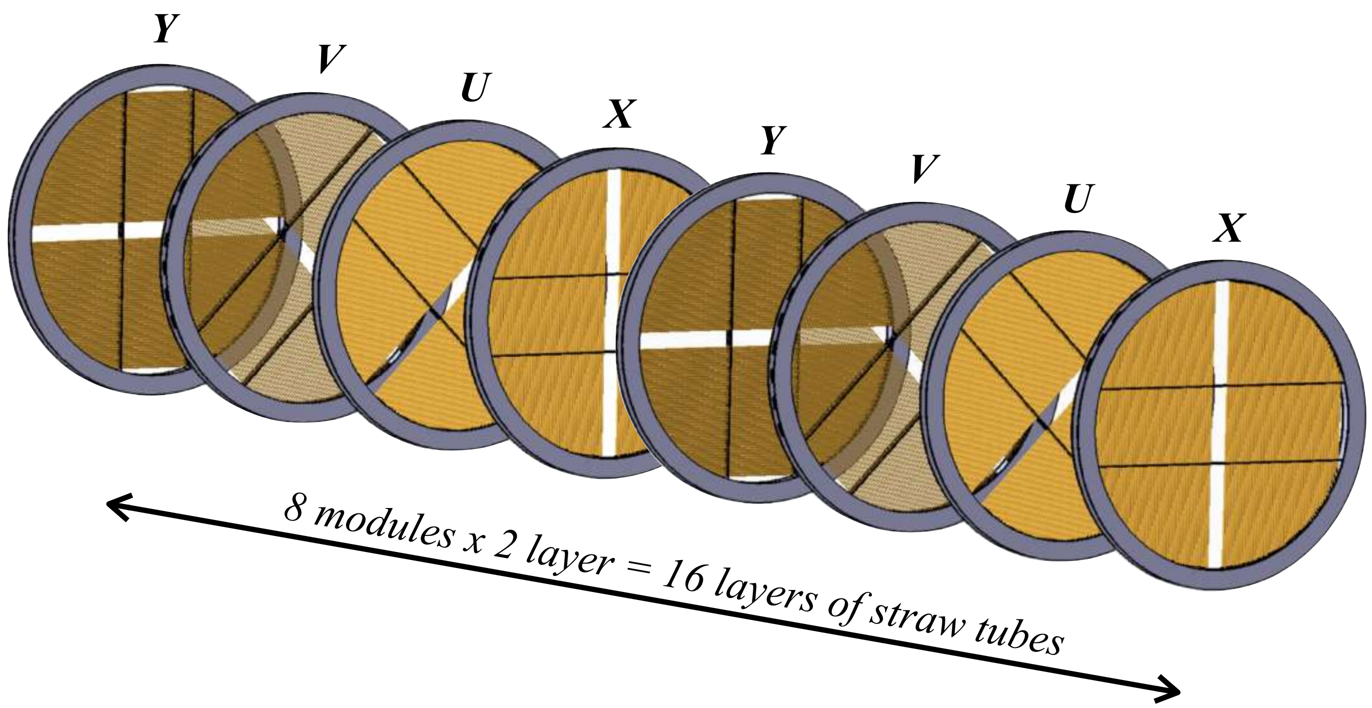

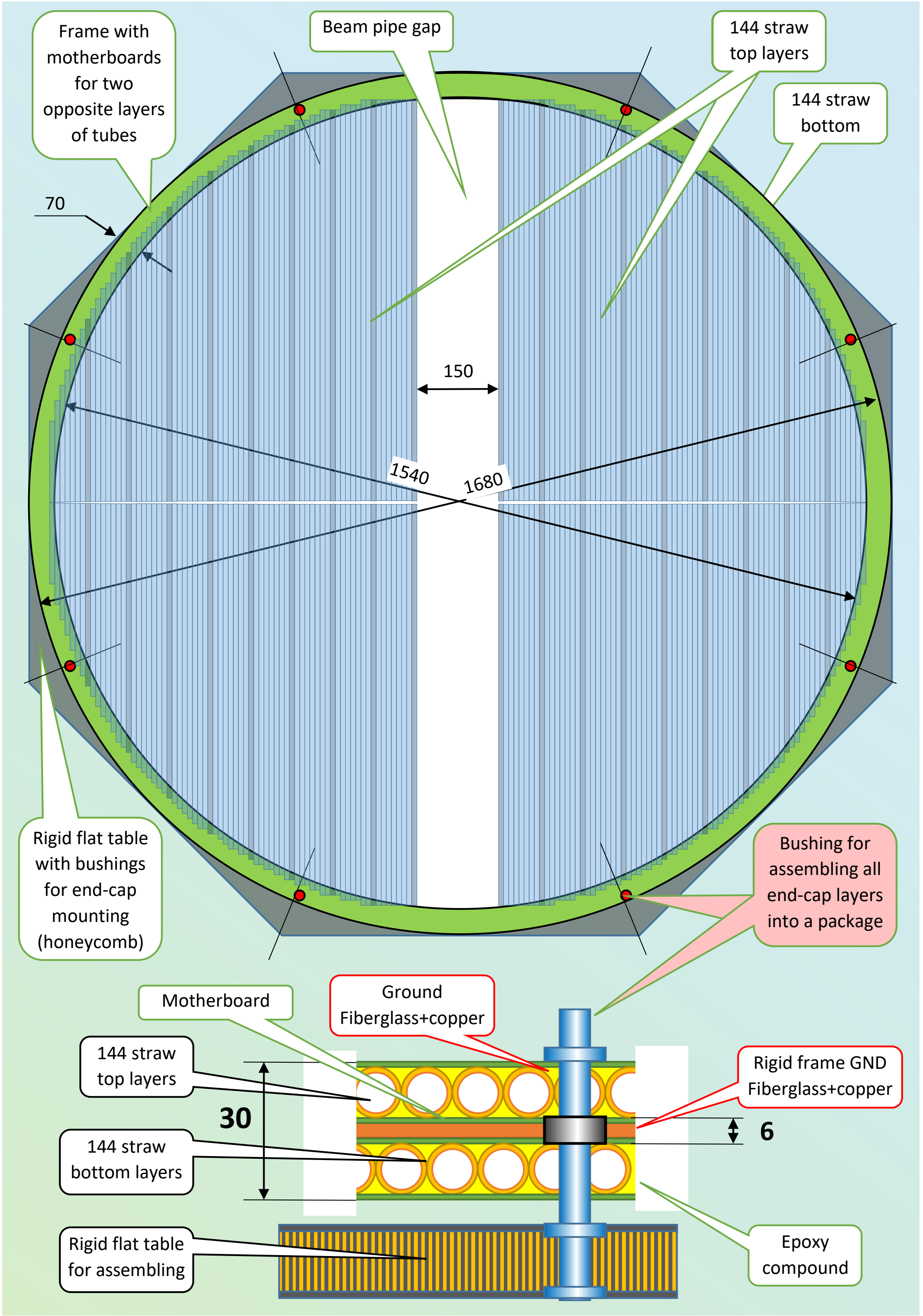

- One ST endcap contains 8 modules: *X*, *+45°*, *-45°*, *Y*
- One module contains 288 tubes in total, which are arranged in two layers shifted by half a tube
- Total number of tubes in two endcaps is

  $$288 \text{ tubes} \times 16 \text{ modules} \times 2 \text{ endcaps} = 9216 \text{ tubes}$$

- The thickness of one module is 30 mm
- Eight coordinate planes are mounted together on a rigid flat table to form a 240 mm thick rigid block
- One straw is made by winding two "kapton" tapes forming a tube with $\varnothing = 9.56$ mm

Silicon Vertex Detector (SVD)

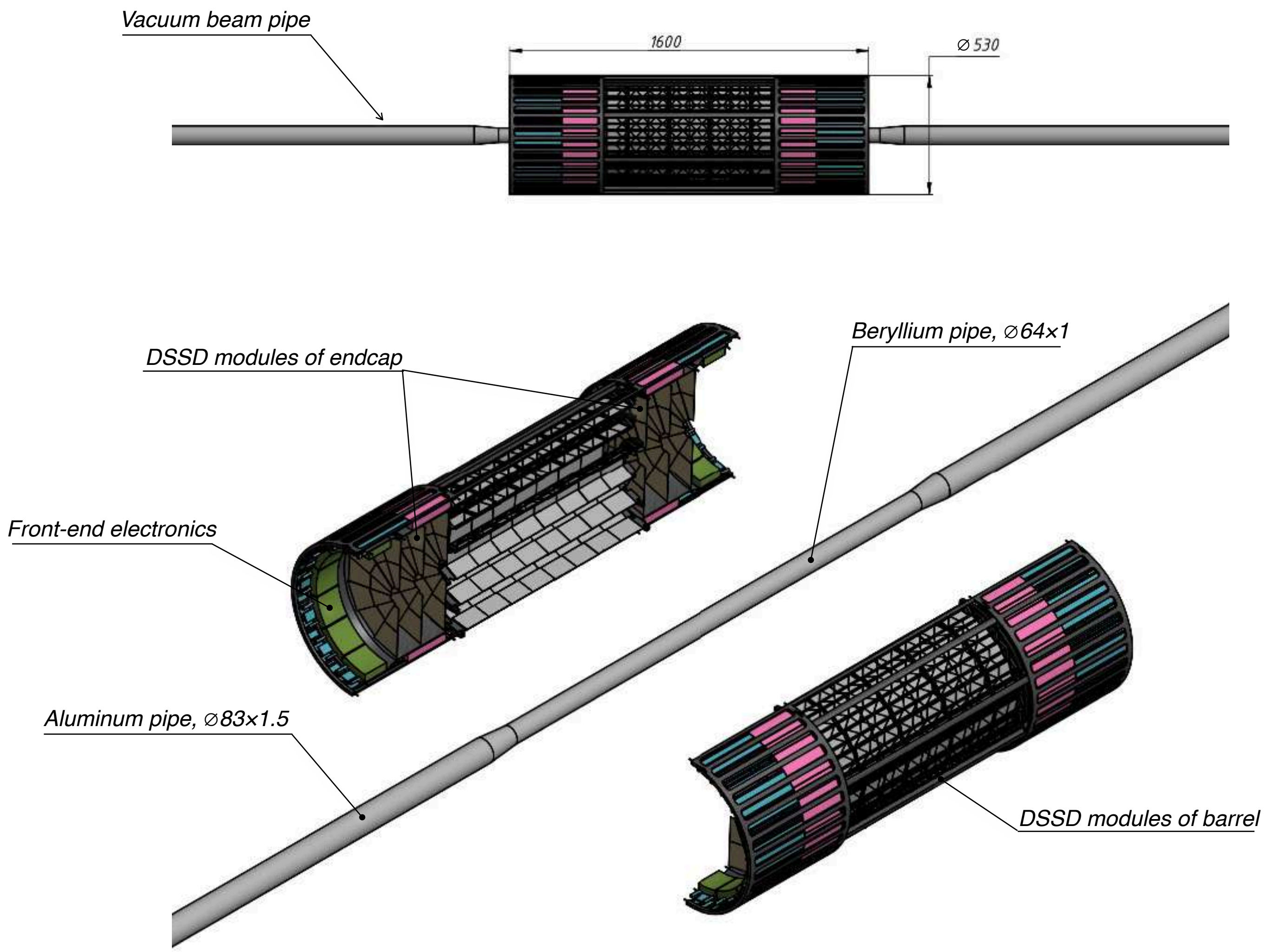

- Silicon Vertex Detector (SVD) by 2035
  - Double-Sided Silicon Detector (DSSD), strip readout, σ=28 μm
  - Monolithic Active Pixel Sensors (MAPS), pixel readout, σ=5 μm
- MicroMegas (MM) detector by 2028
  - Temporary solution while waiting for SVD
  - Strip readout, σ=150 μm
- Detector will be divided into halves, which will be assembled separately
- Once VD is closed it will form a single module with the beam pipe. The detector will not touch the pipe to avoid heat transfer

Transverse momentum resolution

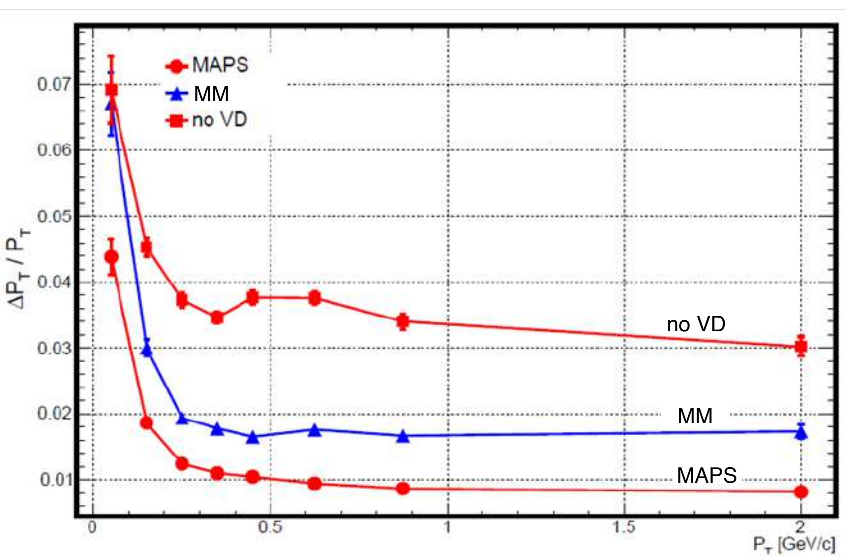

Distance between production and decay vertex

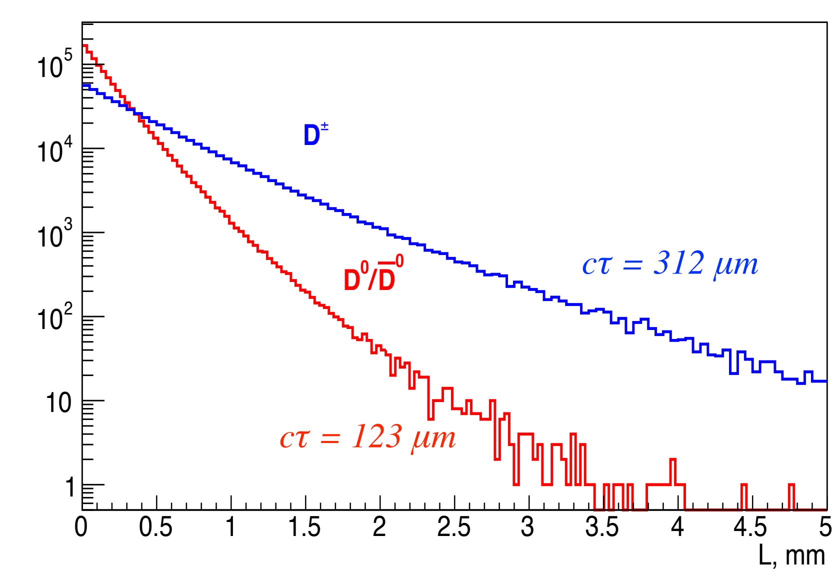

D0 → π^+ + K^- : secondary vertex z-resolution

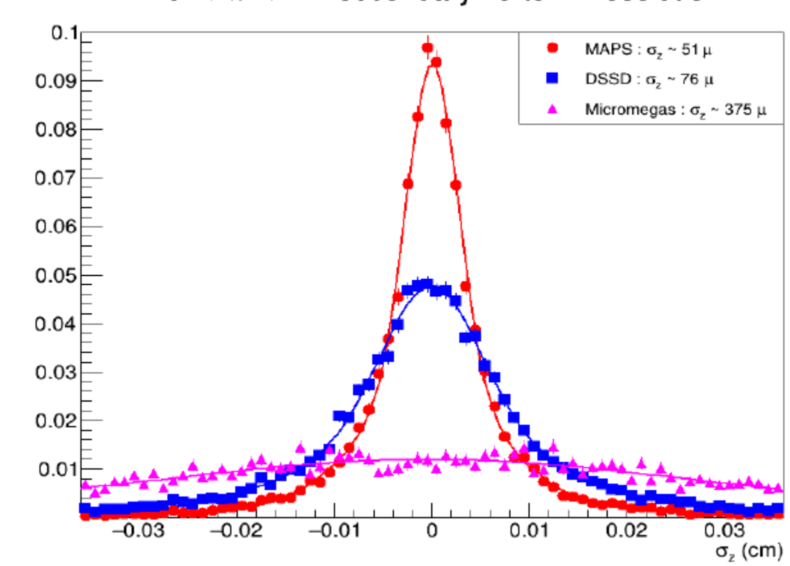

Detectors for local polarimetry and luminosity control

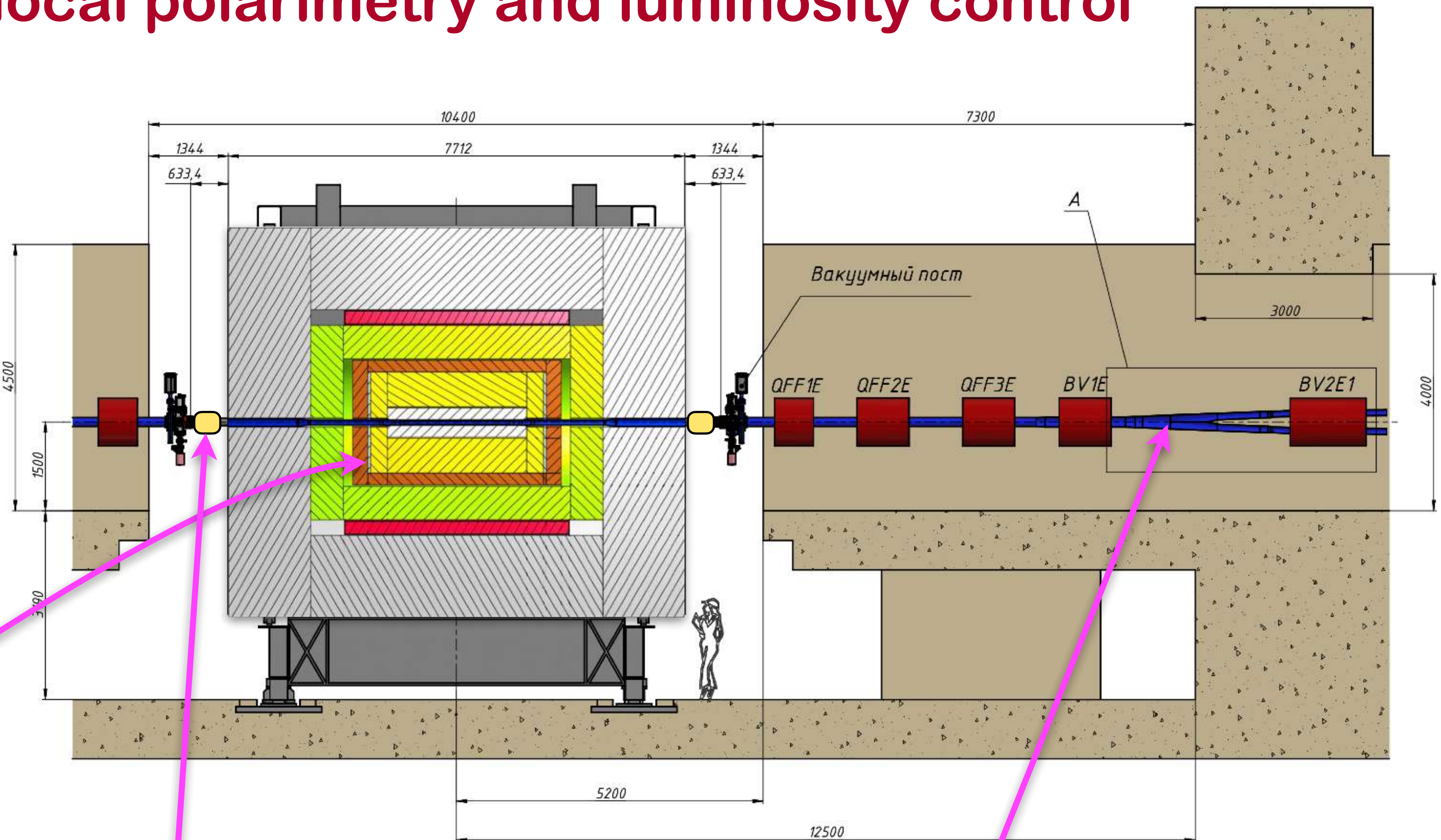

Beam-Beam Counter (BBC)
Plastic scintillator tiles
z = ±1.4m

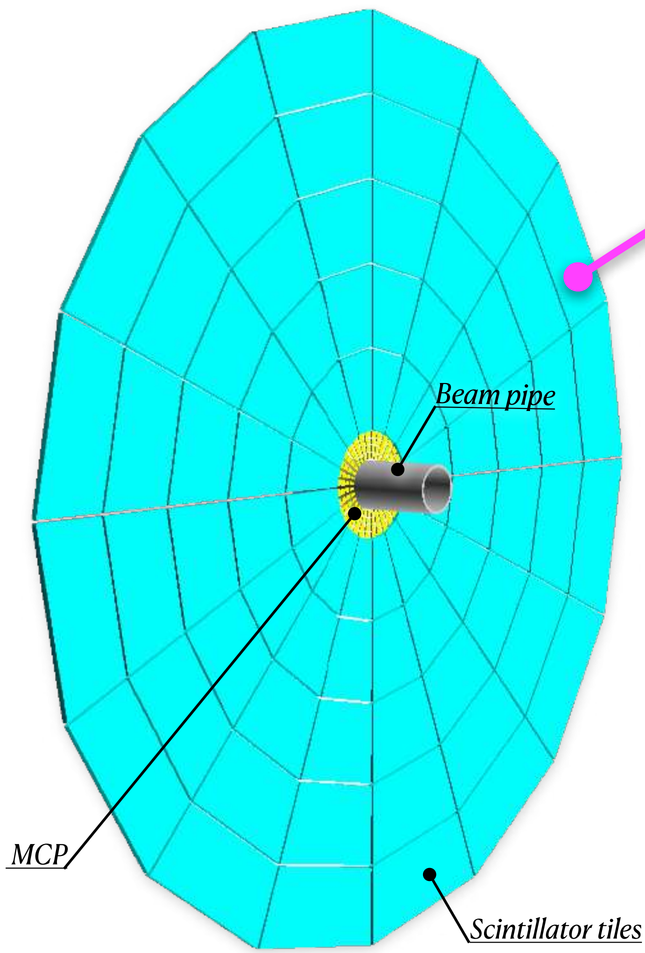

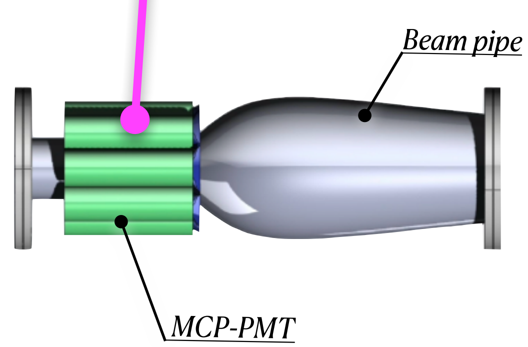

Zero Degree Calorimeter (ZDC)
Sandwich: scintillator pixels / Tungsthen

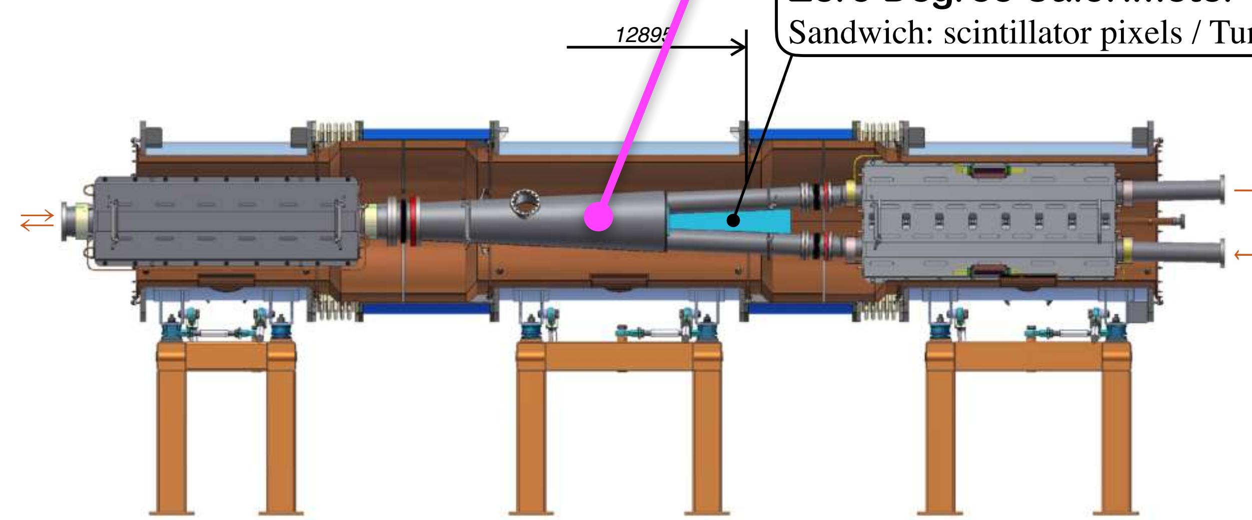

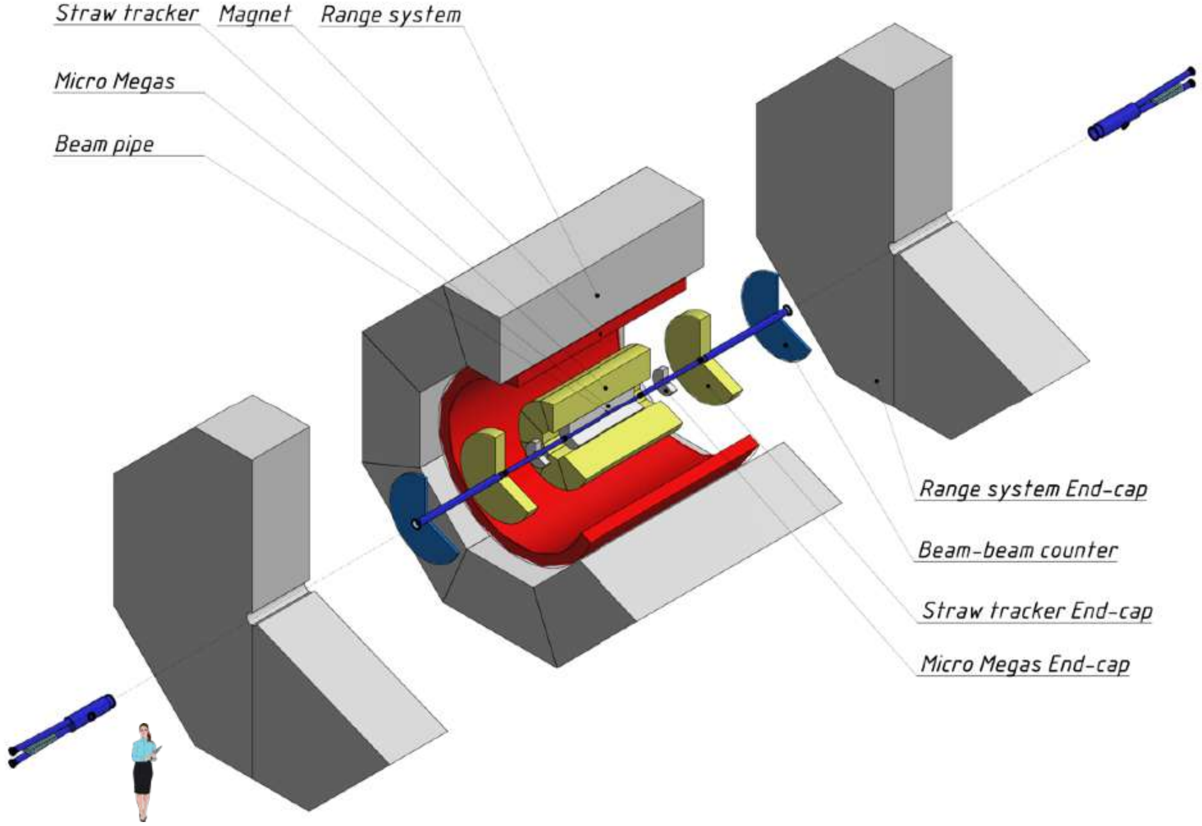

First stage of experiment by 2028

- Basic set of subsystems
  - RS, Straw, MM, and Magnet
  - BBC, MCP, ZDC
- No PID detector (TOF, FARICH), no ECal, no SVD
- p-beam: $\sqrt{s} \lesssim 15$ GeV, $\mathcal{L} \lesssim 10^{30}$ $s^{-1}cm^{-2}$

Fully assembled setup

- p-beam: $\sqrt{s}$=27 GeV, $\mathcal{L}=10^{32}$ $s^{-1}cm^{-2}$

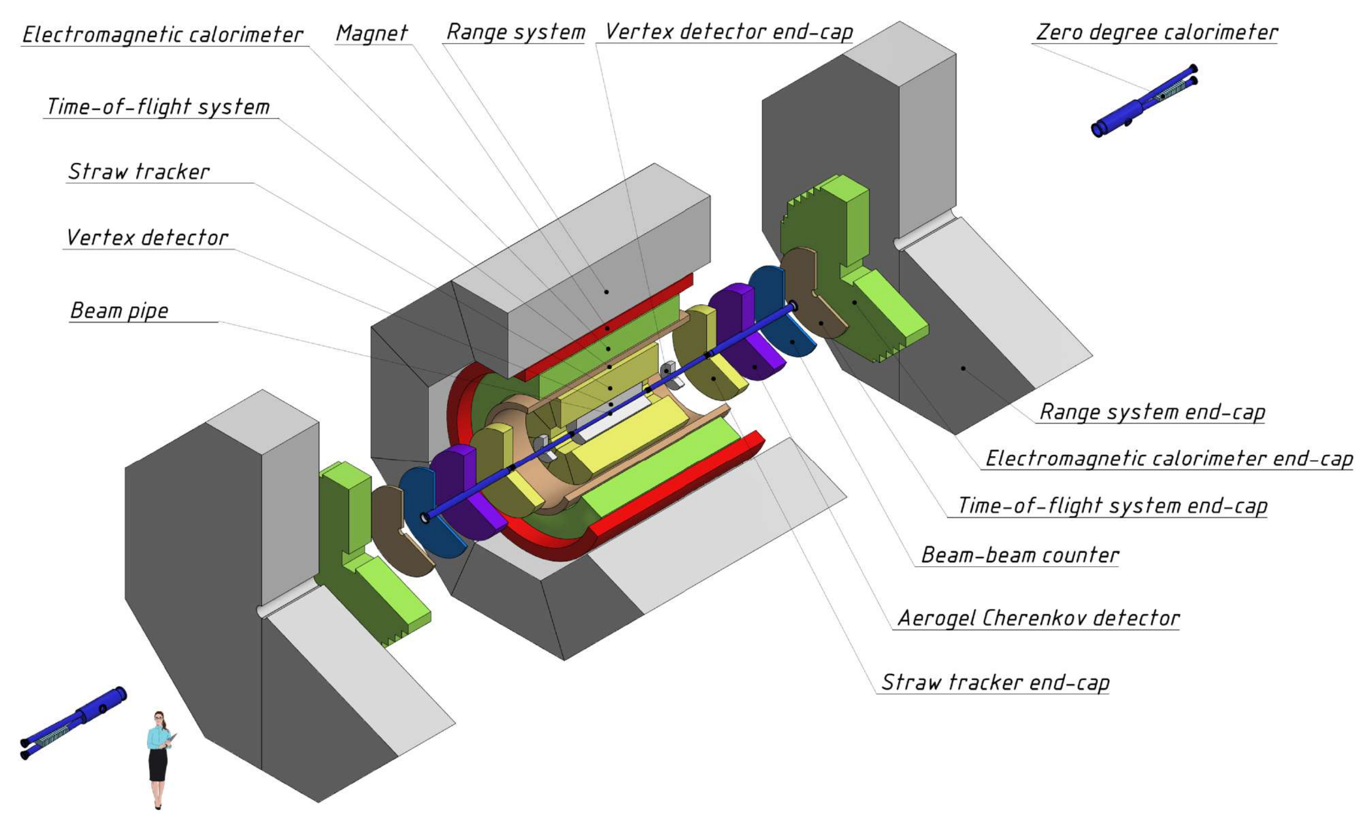

Physics program of SPD

Transverse momentum-dependent (TMD) parton distributions

Tomographic 3D-imaging of proton and deuteron in momentum space. It probes the correlation between the proton spin and the spin and transverse motion of partons. It will requires the maximum energy 27GeV and maximum luminosity of the beam.

gluon TMD

quark TMD

Measurement of differential cross sections and azimuthal single or double spin asymmetries in

gluon induced processes: charmonia, open charm and prompt photon production.

processes involving light hadrons: $\pi^{\pm,0}$, $K^{\pm,0}$, p, $\bar{p}$, n, η, Λ.

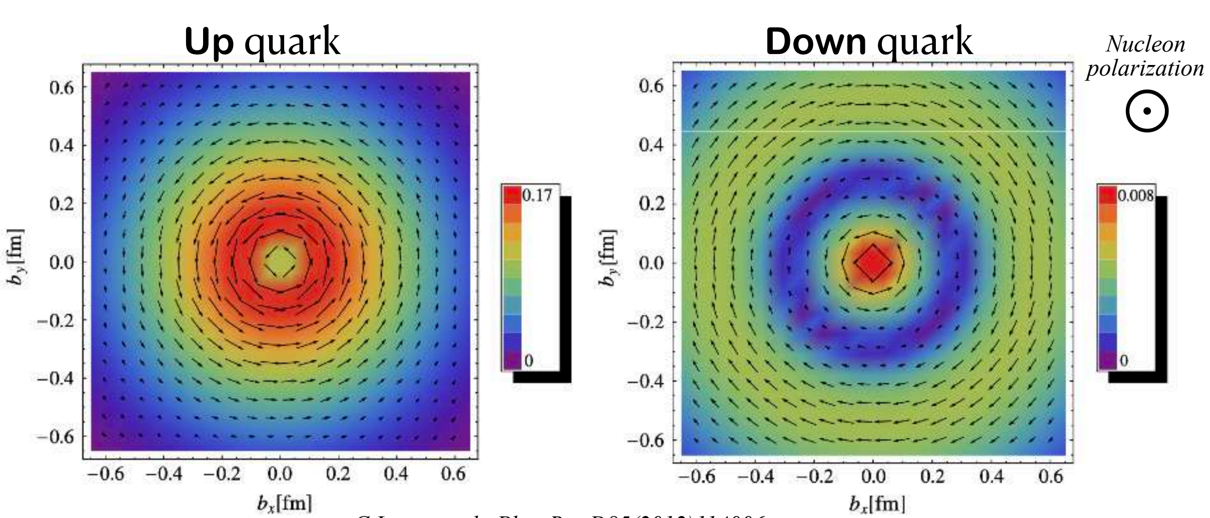

C.Lorce et al., Phys.Rev.D85(2012)114006
Distributions of quarks calculated in light-cone constituent quark model (LCCQM)

QCD in intermediate region

First stage of the experiment with a partially equipped detector and lower energy ≲15GeV and lower luminosity. Physics of the transition region from hadron to quark-gluon degrees of freedom in collisions of free nucleons or lightest nuclei.

- Spin effects in pp, pd and dd (quasi-) elastic scattering
- Studying periphery of the nucleon in diffractive scattering
- Spin effects in hyperons production
- Multi-quark correlations (diquarks, fluctons) and exotic hadron state production
- Light vector meson and charmed meson production near threshold
- Color transparency in nucleons and meson production
- Hypernucei production $d + d \to K^+ + K^- + {}^{4}_{\Lambda\Lambda}n$
- Antiproton production for Dark Matter search
- Test of discrete P and T symmetries
- …

Transverse momentum-dependent (TMD) distributions

- 3D partonic structure of hadron in momentum space (coordinate position of partons is obtained from GPD)
- Transverse motion of quarks results in correlations between the orbital angular momentum and the spin of quarks for nucleons at different polarization states
- TMDs give rise to spin and azimuthal asymmetries

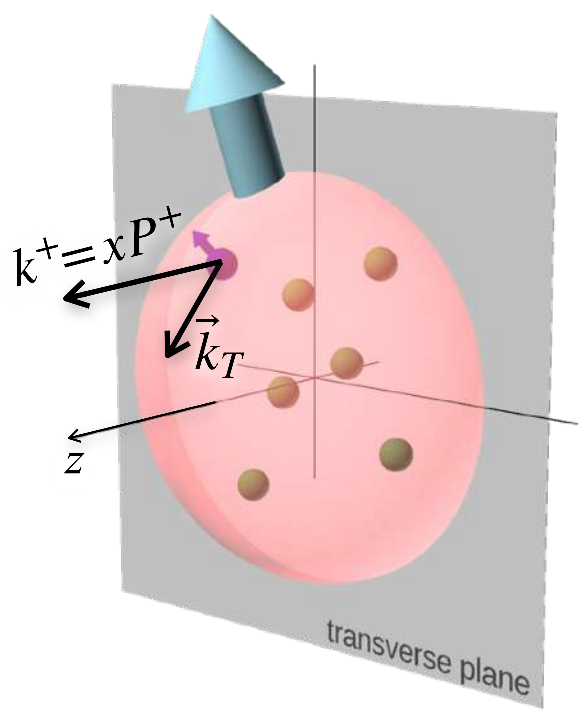

$\vec{k}_\perp$ and $\hat{z}$ are vectors

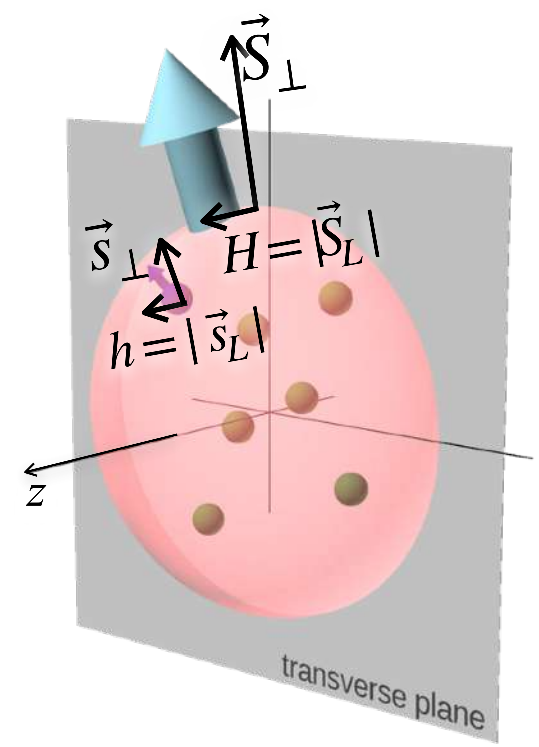

h and H are pseudoscalars

$\vec{S}_\perp$ and $\vec{s}_\perp$ are axial vectors

- Hadronic tensor is decomposed into a set of basis tensors multiplied by *scalar* structure functions (TMDs)
- One needs to find out the basis tensors assuming hermiticity, parity and time-reversal invariances.
- Only 8 independent combinations to construct a *scalar* up to terms quadratic in k_T => Leading twist distributions (densities) in the context of parton model

Transverse momentum-dependent (TMD) parton distributions

Independent of $\vec{k}_\perp$

Number density	Helicity	Transversity
$\mathbb{1}$	hH	$\vec{s}_\perp \cdot \vec{S}_\perp$
$\times\, f_1(x, k_T^2)$	$\times\, g_{1L}(x, k_T^2)$	$\times\, h_1(x, k_T^2)$

Product of pseudo-scalar and axial vector

Worm gear T	Worm gear L
$h\,(\vec{k}_\perp \cdot \vec{S}_\perp)$	$H\,(\vec{k}_\perp \cdot \vec{s}_\perp)$
$\times\, g_{1T}(x, k_T^2)$	$\times\, h_{1L}^{\perp}(x, k_T^2)$

(h and H are pseudoscalars) + ($\vec{k}_\perp$ and $\hat{z}$ are vectors) +
($\vec{S}_\perp$ and $\vec{s}_\perp$ are axial vectors) + hermiticity, parity, time-reversal invariances.
Only 8 independent combinations up to terms quadratic in $\vec{k}_\perp$

Triple product (T-odd)

Sivers function	Boer-Mulders function
$\vec{S}_\perp\,(\vec{k}_\perp \times \hat{z})$	$\vec{s}_\perp\,(\vec{k}_\perp \times \hat{z})$
$\times\, f_{1T}^{\perp}(x, k_T^2)$	$\times\, h_1^{\perp}(x, k_T^2)$

2-nd power in $\vec{k}_\perp$

Pretzelosity

$$2\,(\vec{S}_\perp \cdot \vec{k}_\perp)(\vec{s}_\perp \cdot \vec{k}_\perp) - \vec{k}_\perp^2(\vec{S}_\perp \cdot \vec{s}_\perp)$$

$$\times\, h_{1T}^{\perp}(x, k_T^2)$$

Transverse momentum-dependent (TMD) parton distributions

Nucleon polarization		Quark polarization: Unpolarized, f	Longitudinal, g	Transvers, h
	Unpolarized	Number density 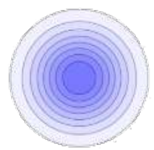 $\sim\mathbb{1}$		Boer-Mulders 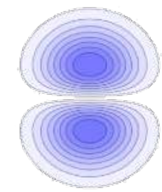 $\sim h\,(\vec{k}_\perp \cdot \vec{S}_\perp)$
	Longitudinal		Helicity 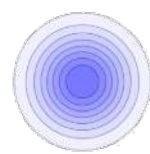 $\sim hH$	Worm-Gear L 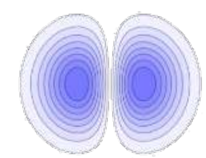 $\sim H\,(\vec{k}_\perp \cdot \vec{s}_\perp)$
	Transvers	Sivers 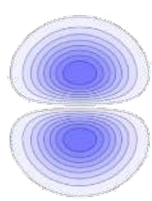 $\sim \vec{S}_\perp\,(\vec{k}_\perp \times \hat{z})$	Worm-Gear T 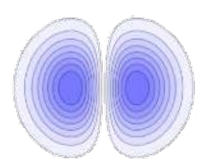 $\sim \vec{s}_\perp\,(\vec{k}_\perp \times \hat{z})$	Transversity 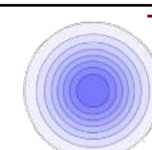 $\sim (\vec{s}_\perp \cdot \vec{S}_\perp)$ Pretzelocity 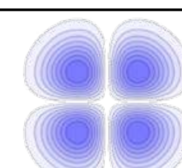 $\sim 2\,(\vec{S}_\perp \cdot \vec{k}_\perp)(\vec{s}_\perp \cdot \vec{k}_\perp) - \vec{k}_\perp^2(\vec{S}_\perp \cdot \vec{s}_\perp)$

- Can be presented as multipoles in momentum space (k_x, k_y)

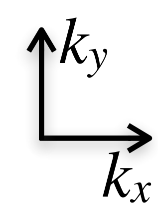

Transverse momentum-dependent (TMD) parton distributions

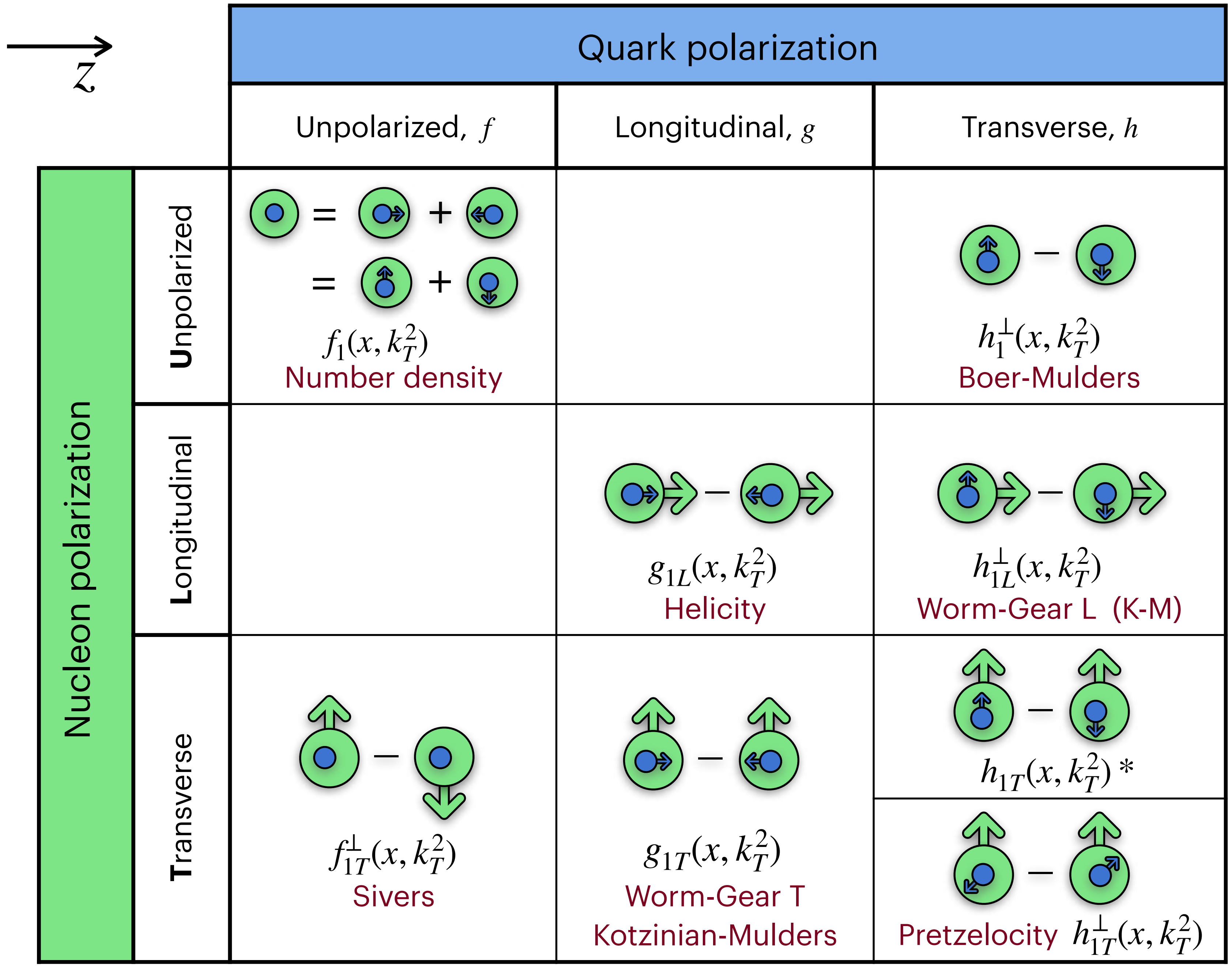

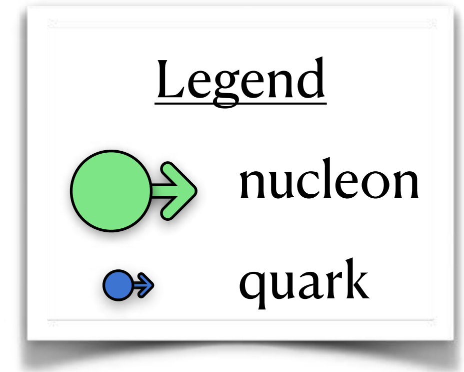

- Subindex "1" indicates the leading twist (twist-2)
- Subindices "L" and "T" indicate polarization of nucleon
- Superscript "$\perp$" indicates the presence of transverse momenta with uncontracted Lorentz indices
- All 8 twist-2 functions can be interpreted as densities
- 16 functions in twist-3. No more probabilistic interpretation

* Transversity: $h_1 = h_{1T} + \frac{k_T^2}{2M^2} h_{1T}^{\perp}$

Sivers effect

Large single-spin asymmetries (SSA) in p↑p→πX processes

- Large SSA observed in many inclusive pion production experiments: $p^{\uparrow}p \rightarrow \pi X$

$$A_N = \frac{d\sigma^{\uparrow} - d\sigma^{\downarrow}}{d\sigma^{\uparrow} + d\sigma^{\downarrow}}$$

- Effect is almost independent of energy
- Sivers effect explains the asymmetry assuming opposite contribution of u and d quarks: $sgn(f_{1T}^{\perp u}) = -\,sgn(f_{1T}^{\perp d})$
  Anselmino et al, hep-ph/9503290, hep-ph/0509035
- Even though effect is large, its description is complicated

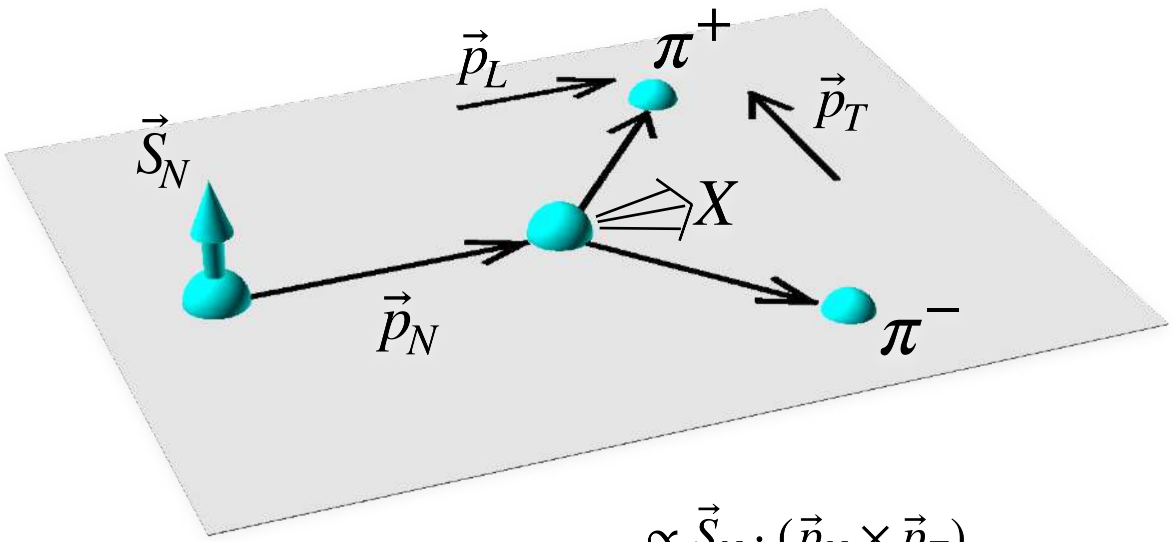

$\propto \vec{S}_N \cdot (\vec{p}_N \times \vec{p}_T)$

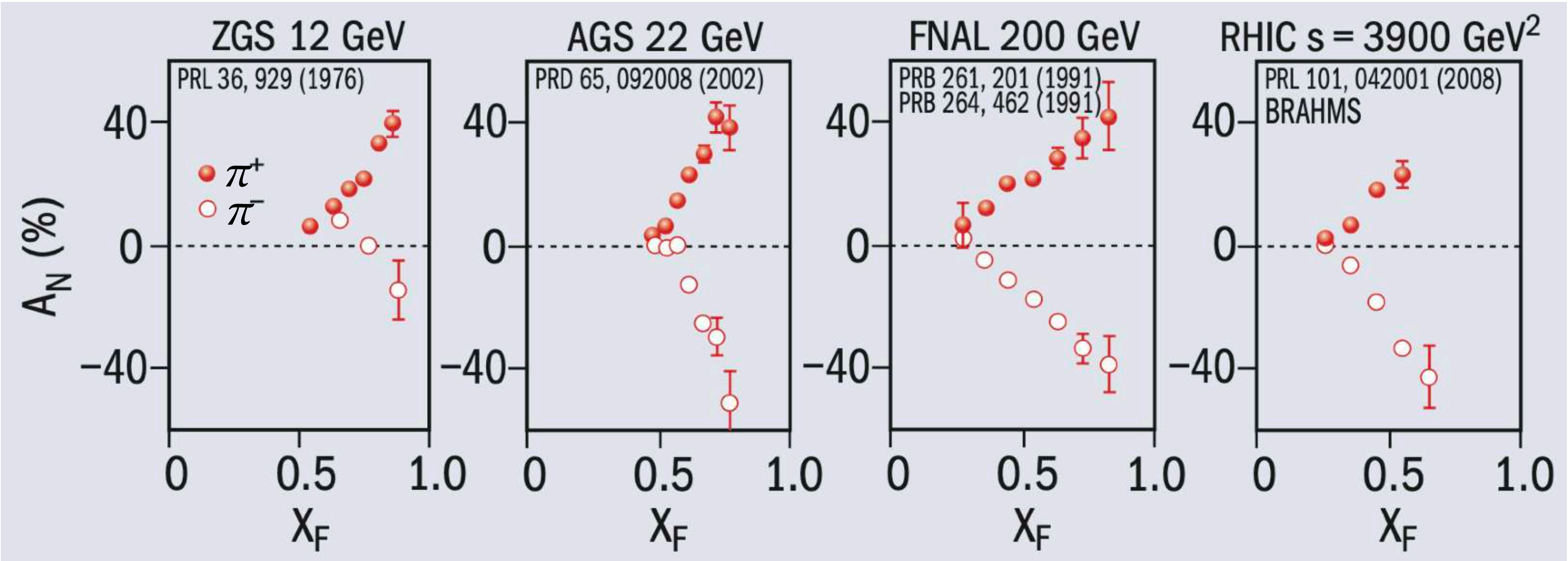

$x_F = 2p_L/\sqrt{s}$

CERN Courier, June 2009

Phenomenological description of SSA of $p^{\uparrow}p \rightarrow \pi X$ processes

- Generalized parton model (GPM) can be considered as a natural phenomenological extension of the usual collinear factorization scheme, with the inclusion of spin and k_T effects through the TMDs

$$\hat{f}_{q/p^{\uparrow}}(x, k_T) = f_{q/p}(x, k_T) + \frac{1}{2}\Delta^N f_{q/p^{\uparrow}}(x, k_T)\ \mathbf{S} \cdot (\hat{\mathbf{P}} \times \hat{\mathbf{k}}_\mathbf{T})$$

- Both Sivers (partonic distributions) and Collins (fragmentation processes) effects contribute to A_N

$$A_N = \frac{[d\sigma^{\uparrow} - d\sigma^{\downarrow}]_{Sivers} + [d\sigma^{\uparrow} - d\sigma^{\downarrow}]_{Collins}}{d\sigma^{\uparrow} + d\sigma^{\downarrow}}$$

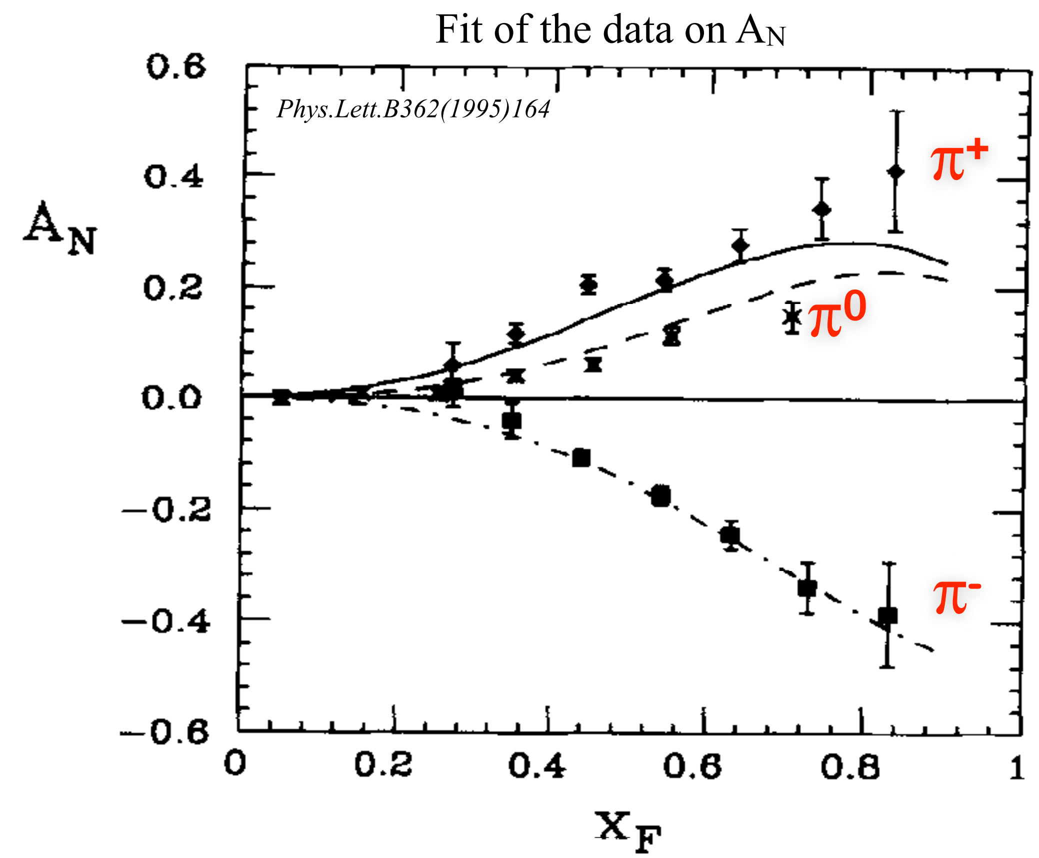

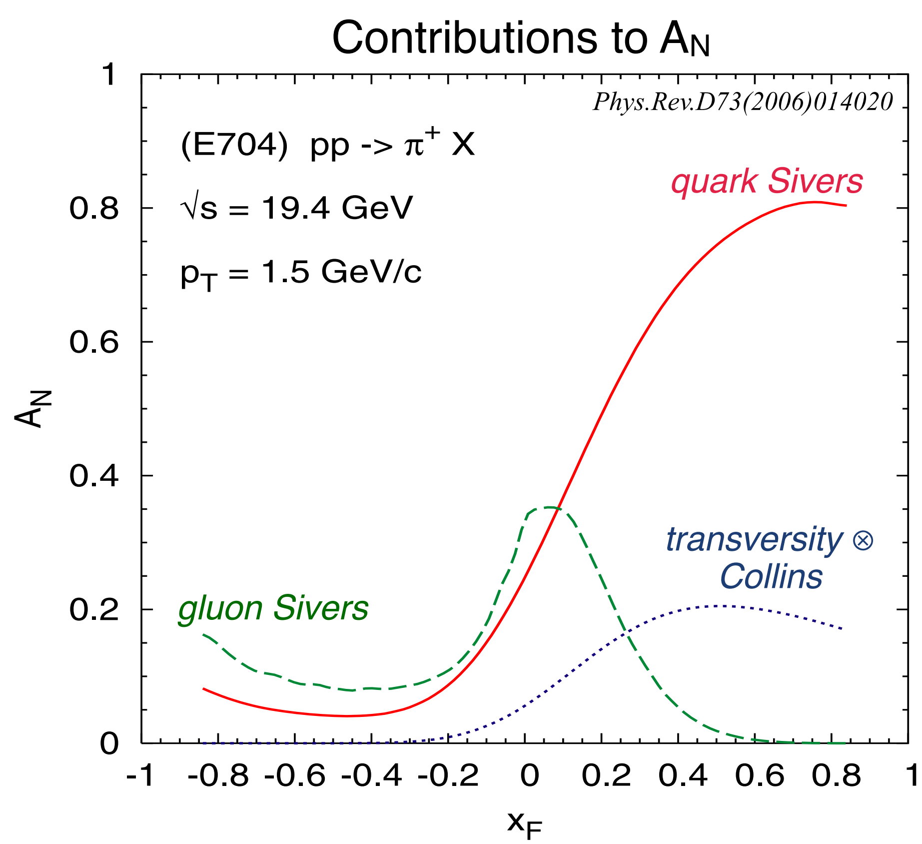

- There is no consistent description (global fit) of all $p^{\uparrow}p \rightarrow \pi X$ data available so far
- Contribution of Sivers mechanism for quarks is largely dominant in the forward region
- Opposite sign of π+ and π- asymmetries can indicate an opposite sign of Sivers function of u and d quarks
- Gluons can be studied in the central and backward regions of x_F
- New data of SPD over a wide rage of p_T and x_F will provide better constrains for the fit

Gluon probes at SPD

Charmonia

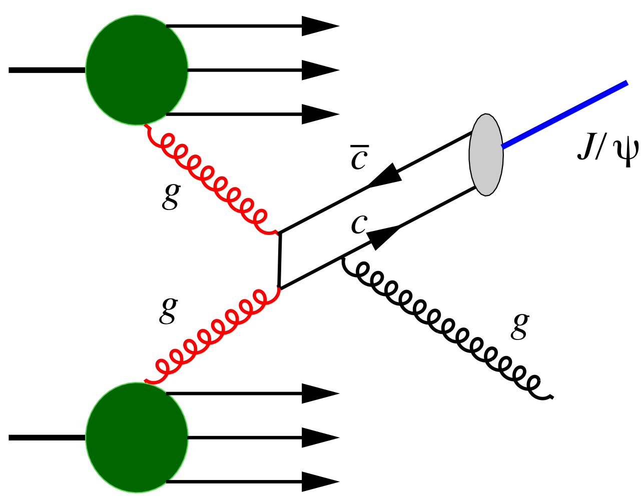

Open charm

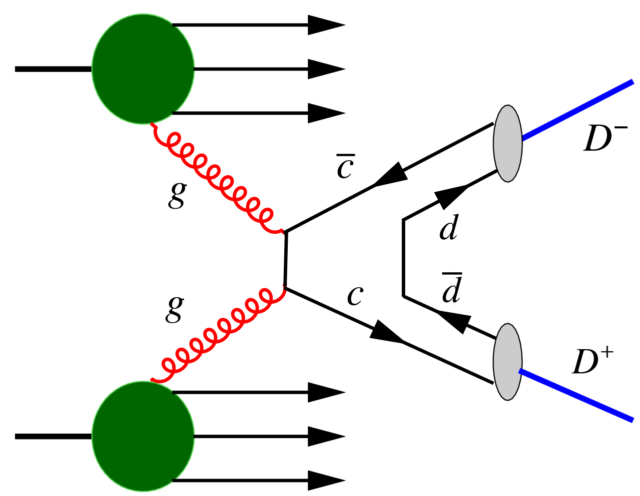

Prompt photon

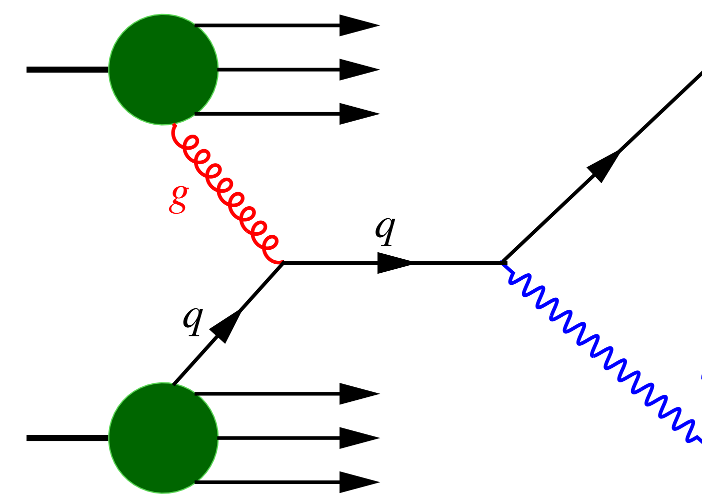

- A.Arbuzov et al., *On the physics potential to study the gluon content of proton and deuteron at NICA SPD*, arXiv:2011.15005
- Measurement of total and differential cross sections (p_T and y dependencies) in charm production to test various models
- Tests of TMD factorization
- Gluon Sivers function via SSA in gluon-induced processes
- Linearly polarized gluons in unpolarized nucleon (B-M function)
- Non-nucleonic degrees of freedom in deuteron
- Gluon polarization Δg with longitudinally polarized beams (fraction of nucleon spin carried by gluons)
- Gluon transversity in deuteron (assuming spin flip ±2, thus does not exist in nucleons)
- …

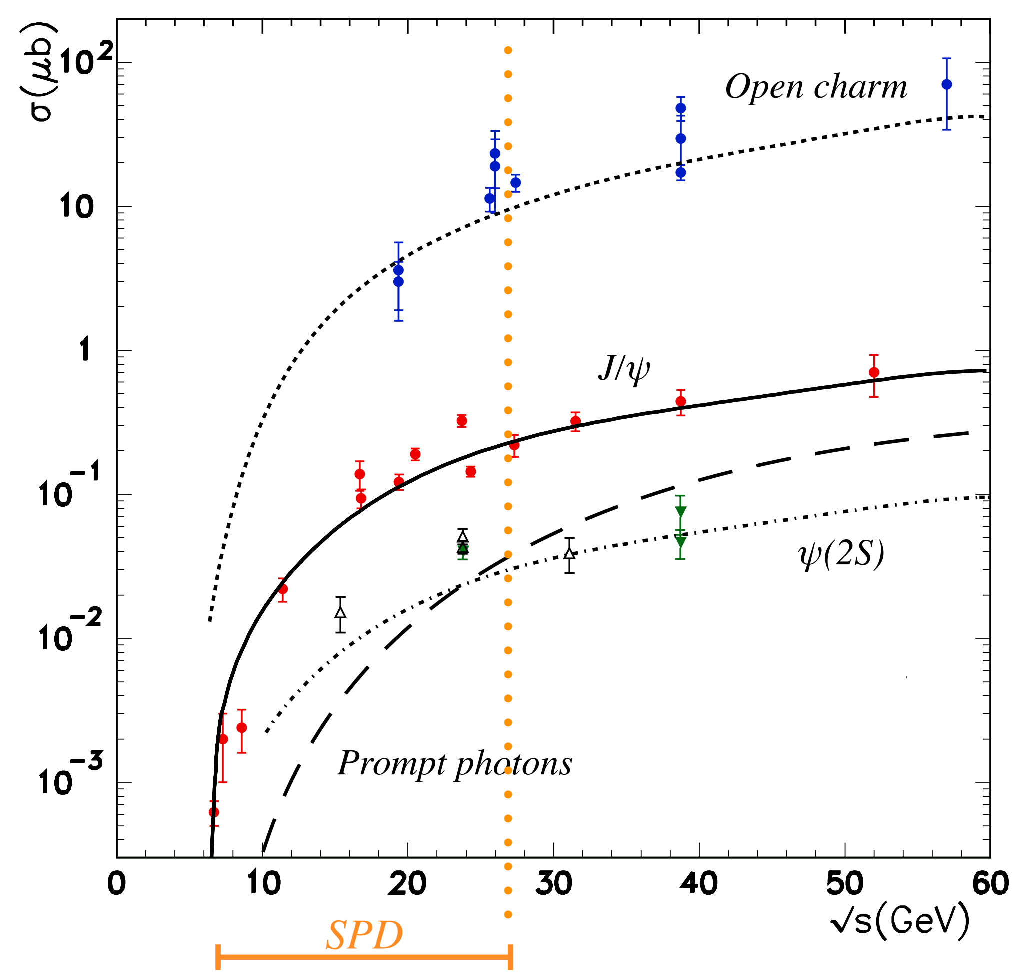

Predictions and statistical uncertainties for the gluon induced asymmetries

- GPM model prediction at √s=27 GeV for data taking for 10^7 s with products produced in the detector acceptance
- Two approaches describing the hadronization stage (refers to the D^0 and J/ψ production)
  - Non-Relativistic QCD factorization (NRQCD)
  - Improved Color-Evaporation Model (ICEM)
- Prompt photon production is a clean probe to study the Sivers DF and twist-3 correlation functions because it proceeds without fragmentation ⇒ is exempt from the Collins effect

d'Alesio GSF parametrization

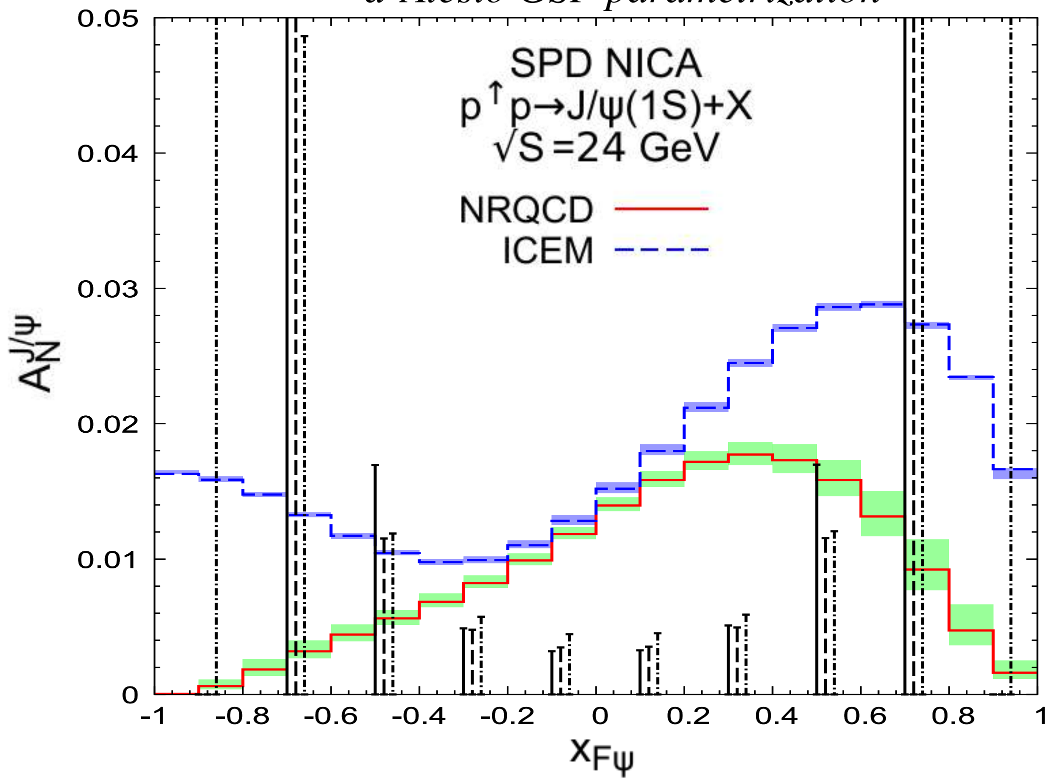

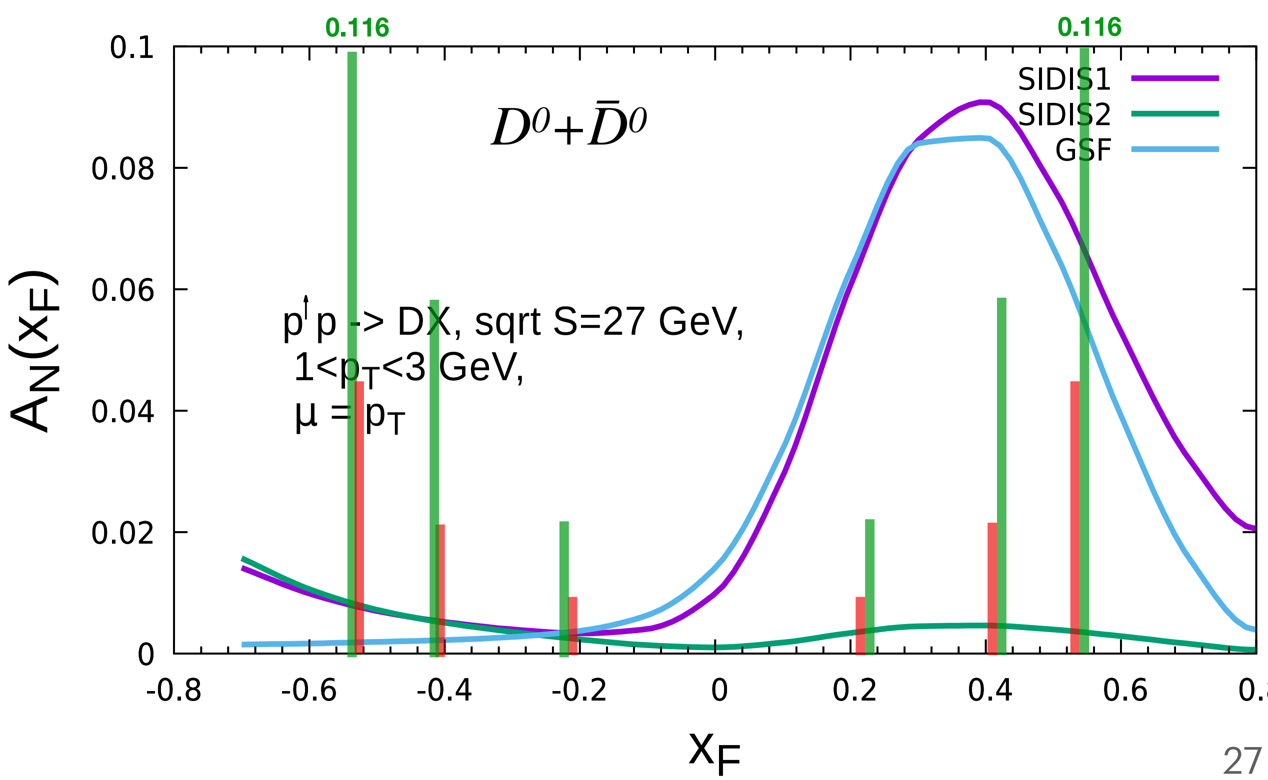

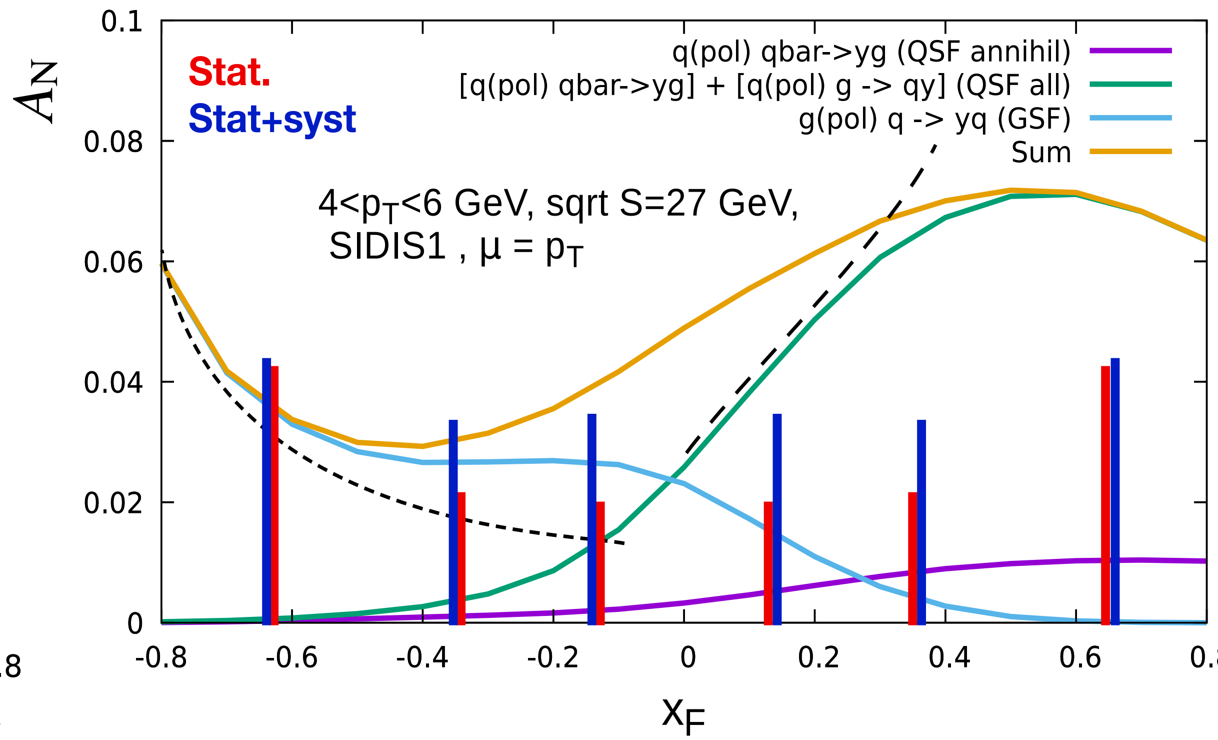

Conclusions

- NICA collider will start operation at JINR Dubna in 2024
  - CM energy scan from few GeV to 27 GeV in *pp* mode
  - Measurements with *pp*, *pd* and *dd* beams
  - All configurations for the beam polarization: U, L, T
- SPD (Spin Physics Detector) is a universal facility with the primary goal to study unpolarized and polarized gluon content of *p* and *d*
  - Main probes: charmonia, open charm and prompt photons
  - 4π detector will be equipped with silicon detector, straw tracker, TOF and FARICH for PID, calorimetry, muon system and monitoring detectors
- Technical Design Report was released at the beginning of this year
- More information could be found at http://spd.jinr.ru

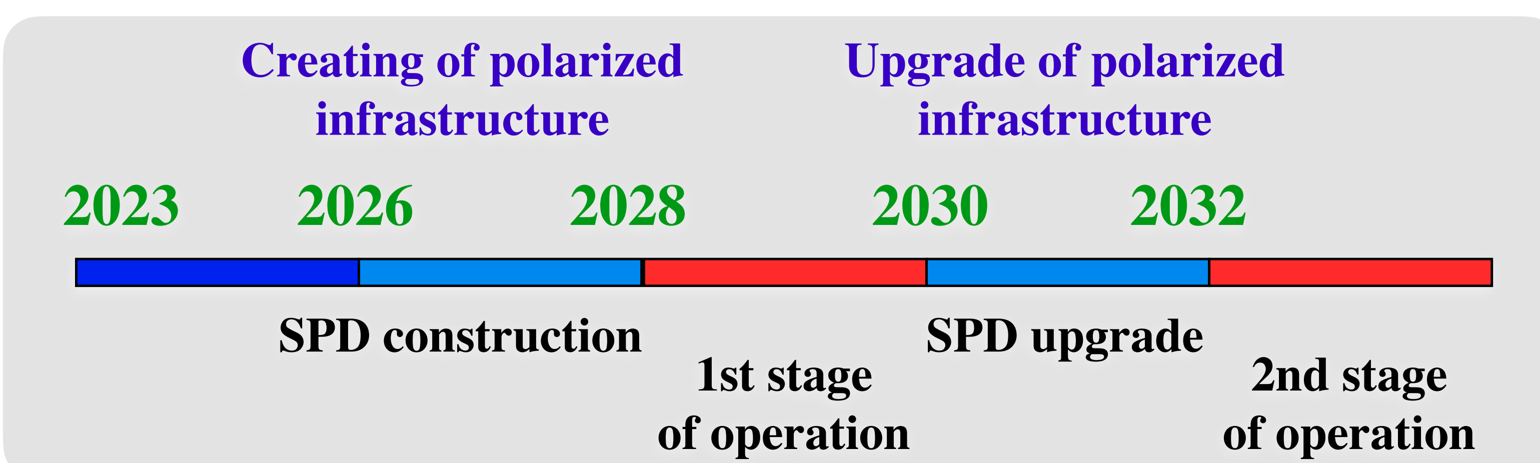

backup

Nuclotron

It started operating ~30 years ago. First SC synchrotron in Europe. Hollow SC cable, cooled by circulating 2-phase helium. It is scheduled to be upgraded by 2030.

Booster

It was mainly introduced for the heavy ion mode (He, Xe, Fe, …, Au). The first run took place in December 2020. In pp mode, is only used to reduce the beam emittance.

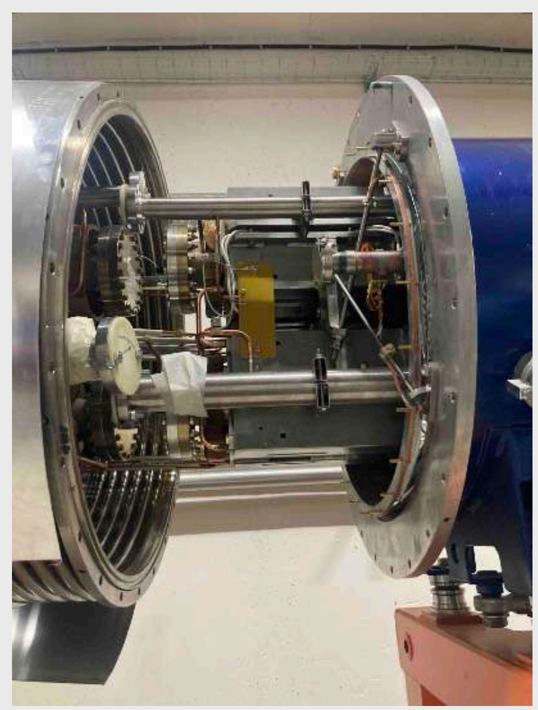

Collider

- In summer 2022, all the dipole magnets were installed in the collider arcs, mechanically adjusted and connected in pairs with each other.
- Installation of engineering infrastructure and straight sections (RF system) is ongoing in 2023.
- Assembly of the Nuclotron-Collider beam transfer line, “cold” and vacuum tests in 2024.

Inner Tracker System of SPD

Micro pattern gaseous detector for the 1-st phase of SPD

(commissioning by 2028)

Cylindrical MicroMegas (MM)

Purpose: temporary replacement for SVD, it serves to improve momentum resolution of tracks by about 2 times 3.5% (ST) →1.7% (ST+MM).

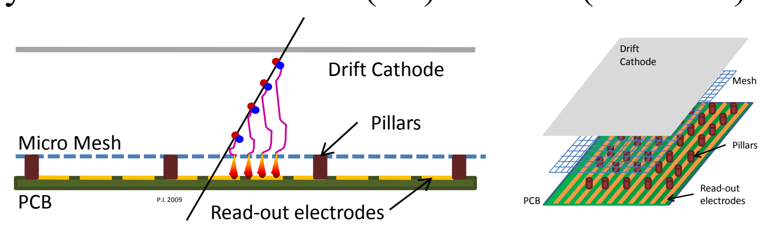

Ionization gap 3 mm, amplification gap 120 µm, gas mixture Ar:C_4H_{10} = 90:10, gas gain 10^4, pitch size 450 µm, will be manufactured in LNP JINR, ***spatial resolution ~150 µm***.

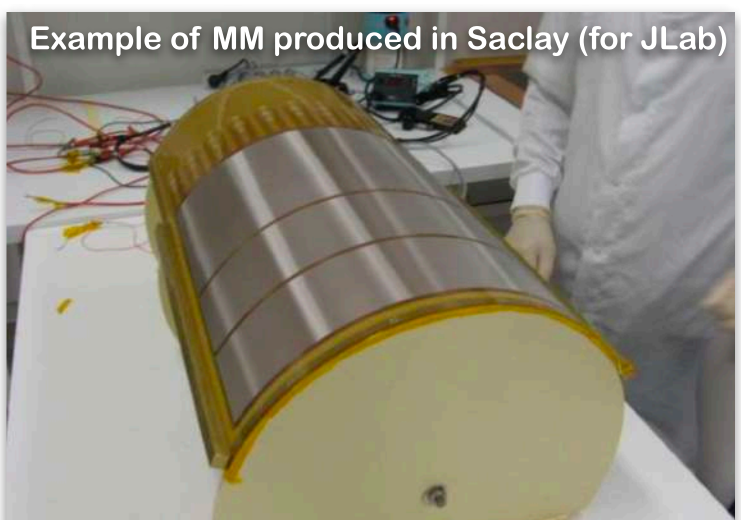
Example of MM produced in Saclay (for JLab)

Bulk technology, cylindrically bent, 3 super-layer (R = 5.5, 11.6, 18.4 cm) with strip tilt angles 0º, ±5º, length of the external layer is 160 cm, readout electronics at two ends, ~14k channels.

Silicon Vertex Detectors (SVD) for the 2-nd phase of SPD

(one of two options, commissioning by 2035)

Double-Sided Silicon Detector (DSSD)

Main purpose of the detector is to reconstruct the position of D-meson decay vertices (σ_z=76 μm).

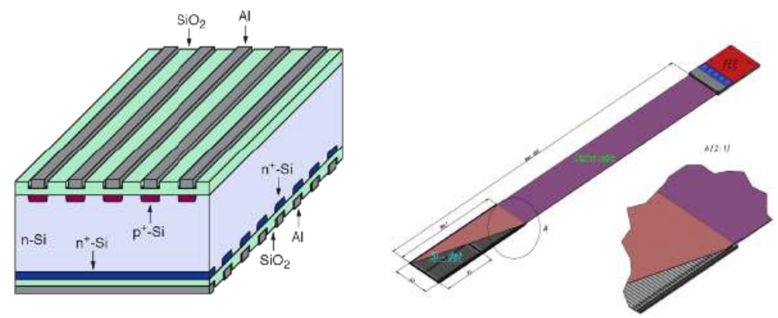

Silicon wafer size 63×93 mm², thickness 300 µm, orthogonal strips on p^+ and n^+ sides, p^+ pitch 95 µm, n^+ pitch 282 µm, produced by ZNTC Russia, ***spatial resolution 27 (81) µm*** for p^+ (n^+) side.

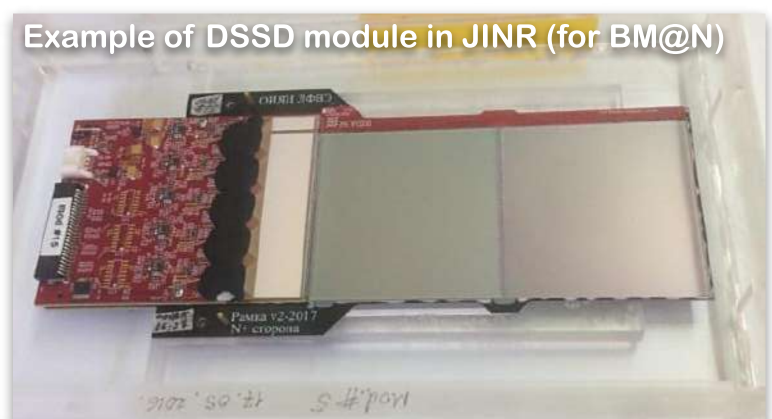
Example of DSSD module in JINR (for BM@N)

DSSD modules are assembled in ladders with carbon fiber support, 3 layers (R=5, 13, 21 cm) in barrel 74 cm long, 3 layers in each endcap, readout electronics at two ends, ~108k channels.

Monolithic Active Pixel Sensors (MAPS)

Main purpose of the detector is to reconstruct the position of D-meson decay vertices (σ_z=51 μm).

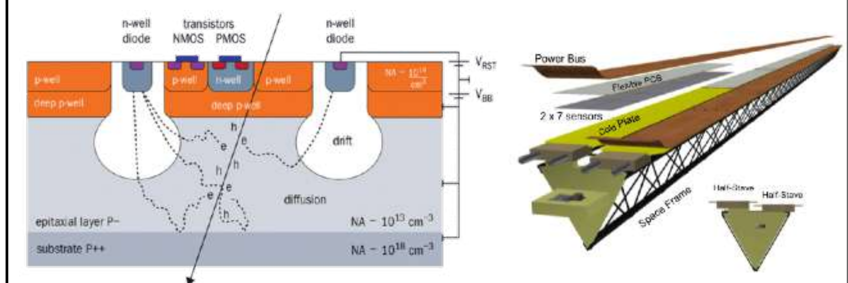

Silicon wafer size 30×15 mm², thickness 50 µm, pitch 28 µm, 512×1024 pixels, sensor and FEE sections are integrated in a single chip, so far is not produced in Russia, ***spatial resolution 5 µm***.

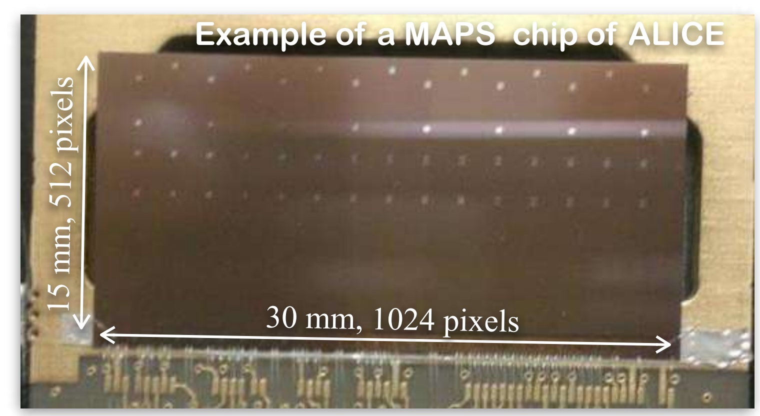

Example of a MAPS chip of ALICE

MAPS chips are assembled in staves with carbon fiber support, 4 layers (R=4, 10, 15, 21 cm) with the external layer 127 cm long, FE electronics is part of the chip, ~10^9 pixels for readout.

Possible studies at the first stage of the NICA collider operation with polarized and unpolarized proton and deuteron beams, *arXiv:2102.08477*

V.V. Abramov[1], A. Aleshko[2], V.A. Baskov[3], E. Boos[2], V. Bunichev[2], O.D. Dalkarov[3], R. El-Kholy[4], A. Galoyan[5], A.V. Guskov[6], V.T. Kim[7,8], E. Kokoulina[5,9], I.A. Koop[10,11,12], B.F. Kostenko[13], A.D. Kovalenko[5], V.P. Ladygin[5], A. B. Larionov[14,15], A.I. L'vov[3], A.I. Milstein[10,11], V.A. Nikitin[5], N. N. Nikolaev[16,26], A. S. Popov[10], V.V. Polyanskiy[3], J.-M. Richard[17], S. G. Salnikov[10], A.A. Shavrin[18,], P.Yu. Shatunov[10,11], Yu.M. Shatunov[10,11], O.V. Selyugin[14], M. Strikman[19,], E. Tomasi-Gustafsson[20], V.V. Uzhinsky[13,], Yu.N. Uzikov[6,21,22,], Qian Wang[23], Qiang Zhao[24,25], A.V. Zelenov[7]*

Model calculation of quark orbital angular momentum

$$L_z^q = \int dx\, d^2\vec{k}_T\, d\vec{b}_\perp\, (\vec{b}_\perp \times \vec{k}_T)_z\, \rho_{LU}(\vec{b}_\perp, \vec{k}_T, x)$$

Wigner distribution of unpolarized (U) quark in a longitudinally (L) polarized nucleon

Light-cone constituent quark model (LCCQM)
C.Lorce, B.Pasquini, X.Xiong, F.Yuan, arXiv:1111.4827

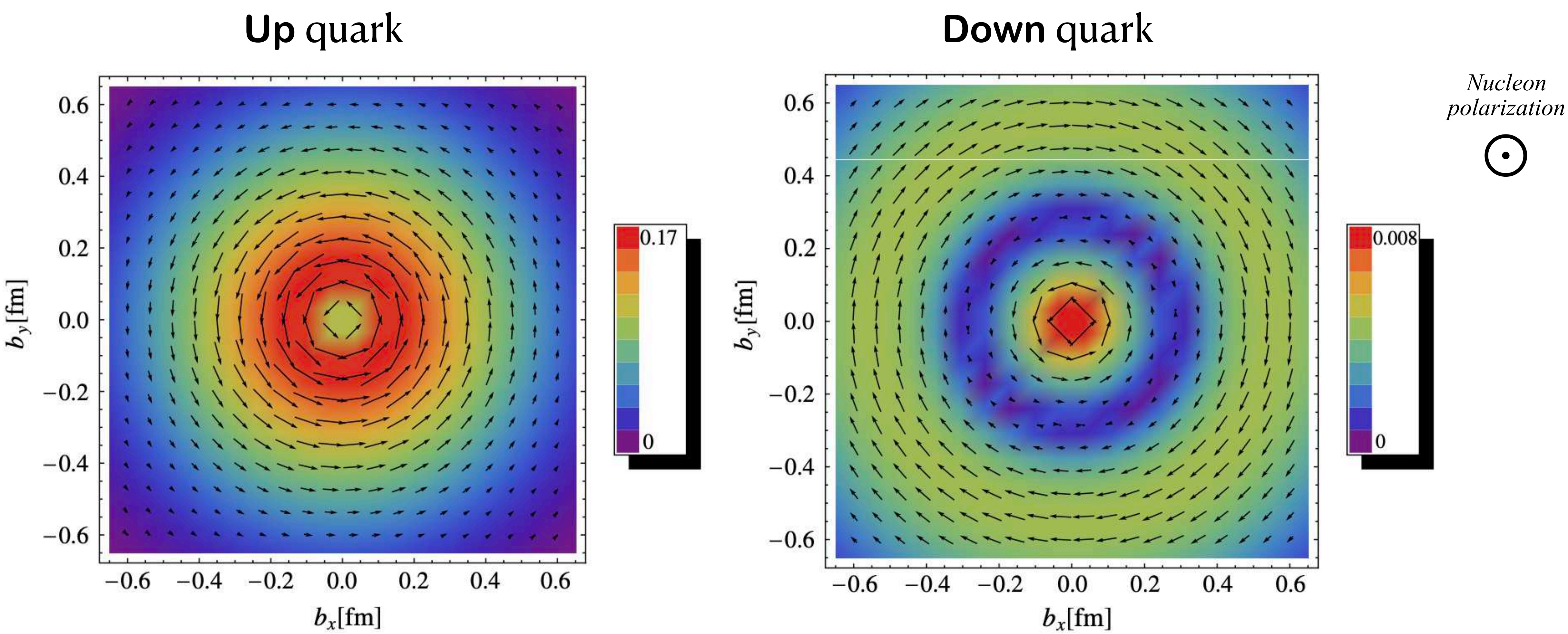

Functions describing the nucleon structure

5D

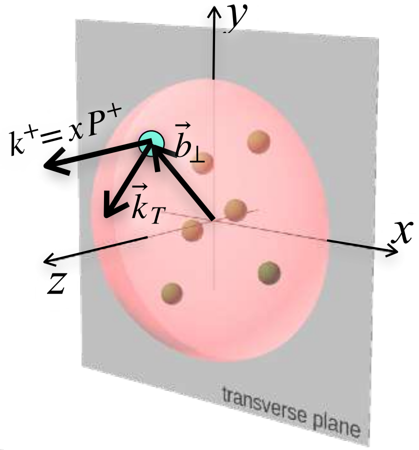

Wigner distribution

$\rho(x, \vec{k}_T, \vec{b}_\perp)$

$\leftarrow FT \rightarrow$
$\xi = 0$

Generalized Transverse Momentum Distributions:

$GTMD(x, \xi, \vec{k}_T, \vec{\Delta}_\perp)$

$\int d^2b_\perp$

$\int d^2k_T$

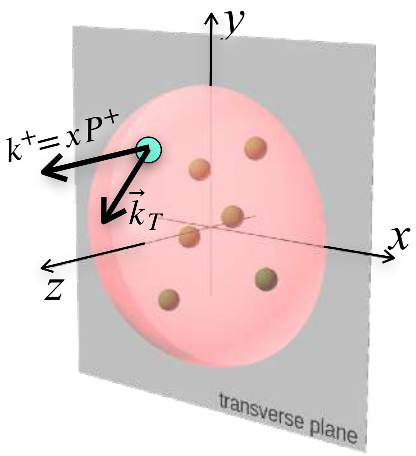

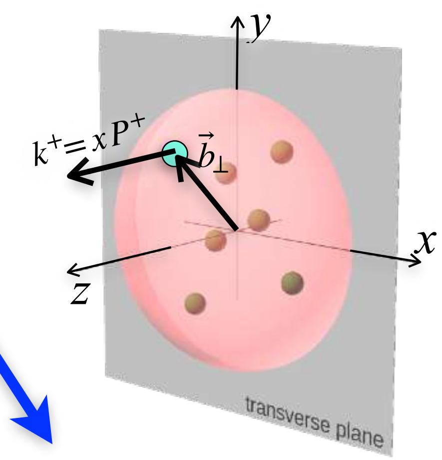

3D

Transverse Momentum Distributions: $TMD(x, \vec{k}_T)$

Generalized Parton Distributions:

$GPD(x, \vec{b}_\perp) \leftarrow FT \rightarrow GPD(x, \vec{\Delta}_\perp) \xleftarrow[\xi = 0]{} GPD(x, \xi, \vec{\Delta}_\perp)$

$\int d^2k_T$

$\int d^2b_\perp$

$\int dx$

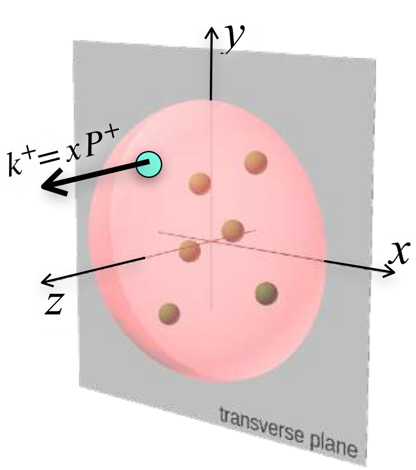

Parton distributions

$PDF(x)$

1D

Form Factors

$F(\vec{b}_\perp)$

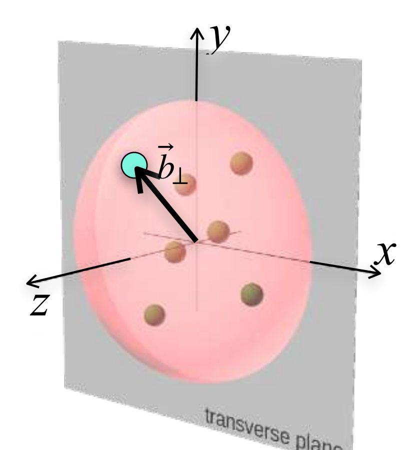

Diehl, arXiv:1512.01328

Generalized Transverse Momentum Distribution (GTMD)

- Average momentum P and momentum transfer to nucleon Δ

$$P = \frac{p + p'}{2}, \qquad \Delta = p' - p$$

- Average momentum fraction of quark: $x = k^+/P^+$

- Fraction of longitudinal momentum transfer to nucleon (skewness)

$$\xi = \frac{p^+ - p'^+}{p^+ + p'^+} = -\frac{\Delta^+}{2P^+}$$

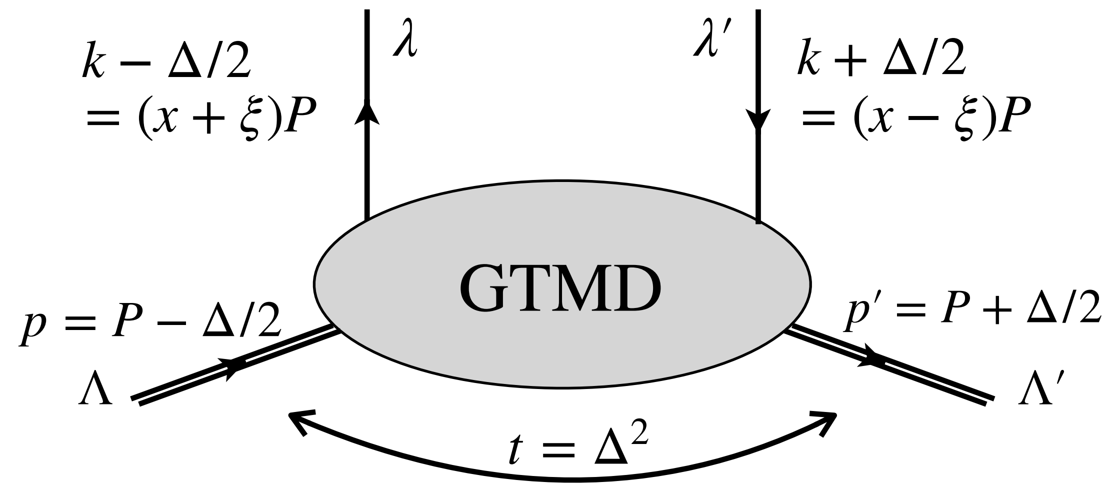

$$\Delta^2 = -\frac{4\xi^2 m^2 + \vec{\Delta}_\perp^2}{1 - \xi^2}$$

- Generalized quark-quark correlator for a spin-1/2 hadron

$$W^{q[\Gamma]}_{\Lambda,\Lambda'} = \frac{1}{2}\int \frac{dz^- d^2\vec{z}_\perp}{(2\pi)^3}\, e^{ik\cdot z}\, \langle p', \Lambda' | \bar{\psi}^q(-\tfrac{z}{2})\, \Gamma\, \mathscr{W}(-\tfrac{z}{2}, \tfrac{z}{2})\, \psi^q(\tfrac{z}{2}) | p, \Lambda \rangle \Big|_{z^+=0}$$

nucleon polarization *quark polarization (Dirac matrices)* *Wilson gauge link*

- Complete parametrization using 16 complex-valued twist-2 GTMDs

$$X(x, \xi, \vec{k}_\perp^2, \vec{k}_\perp \cdot \vec{\Delta}_\perp, \vec{\Delta}_\perp^2; \eta)$$

Meissner, Metz, Schlegel, arXiv:0906.5323

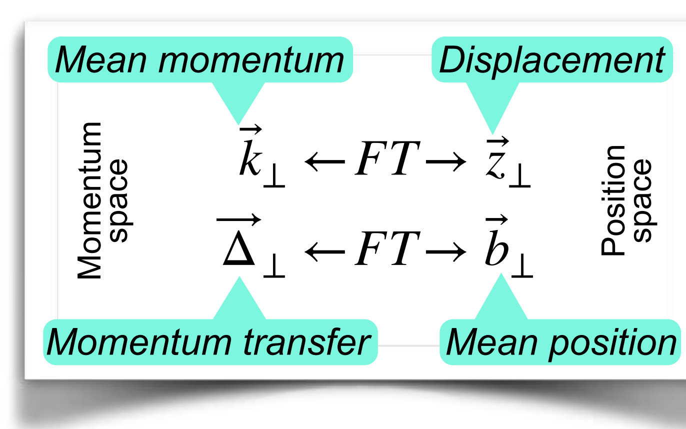

Definitions of OAM
kinetic vs canonical

$GTMD(x, \xi, \vec{k}_T, \vec{\Delta}_\perp)$

Nucleon polarization \ Quark polarization	U	L	T
U	$F_{1,1}$	$G_{1,1}$	$H_{1,1}\ H_{1,2}$
L	$F_{1,4}$	$G_{1,4}$	$H_{1,7}\ H_{1,8}$
T	$F_{1,2}\ F_{1,3}$	$G_{1,2}\ G_{1,3}$	$H_{1,3}\ H_{1,4}$ $H_{1,5}\ H_{1,6}$

16 in twist-2
32 in twist-3
16 in twist-4

$$L_z^{can} = -\int dx\, d^2k_T\, \frac{\vec{k}^2}{M^2}\, F_{1,4}^{\perp}(x, 0, \vec{k}^2, \vec{0}^2)$$

$\xi = 0,\ \vec{\Delta}_\perp = 0$

$\xi = 0,\ \int d^2k_T$

$TMD(x, \vec{k})$

Nucleon polarization \ Quark polarization	U	L	T
U	f_1		$h_1^{\perp}$
L		g_{1L}	$h_{1L}^{\perp}$
T	$f_{1T}^{\perp}$	g_{1T}	$h_1\ h_{1T}^{\perp}$

8 in twist-2
16 in twist-3
8 in twist-4

$GPD(x, \vec{\Delta}_\perp)$

Nucleon polarization \ Quark polarization	U	L	T
U	H		E_T
L		$\tilde{H}$	$\tilde{E}_T$
T	E	$\tilde{E}$	$H_T\ \tilde{H}_T$

8 in twist-2
16 in twist-3
8 in twist-4

$$L_z^{can} = -\int dx\, d^2k_T\, \frac{\vec{k}^2}{2M^2}\, h_{1T}^{\perp}(x\vec{k}^2)$$

$$L_z^{kin} = \frac{1}{2}\int dx\, x[H(x,0,0) + E(x,0,0)] - \frac{1}{2}\int dx\, \tilde{H}(x,0,0)$$

Example of TMD and GPD processes

TMD

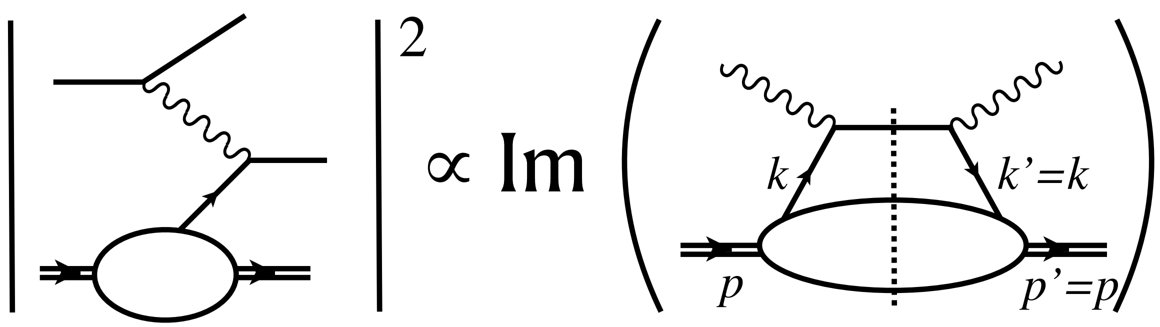

$$\gamma^*(q) + p(p) \rightarrow \gamma^*(q) + p(p)$$

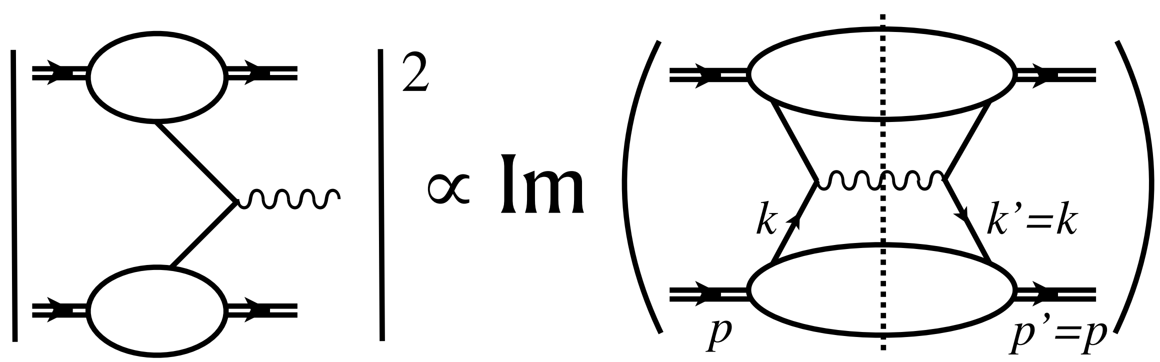

$$p(p_1) + p(p_2) \rightarrow p(p_1) + p(p_2)$$

4-momentum transferred from probe to nucleon

$\Delta = (p'-p)/2 = 0$ *(forward limit)*

Diagonal matrix element of quark-quark operator

$$\langle p, \Lambda | \bar{\psi}^q(-\frac{z}{2}) \Gamma \mathscr{W}(-\frac{z}{2}, \frac{z}{2}) \psi^q(\frac{z}{2}) | p, \Lambda \rangle$$

GPD

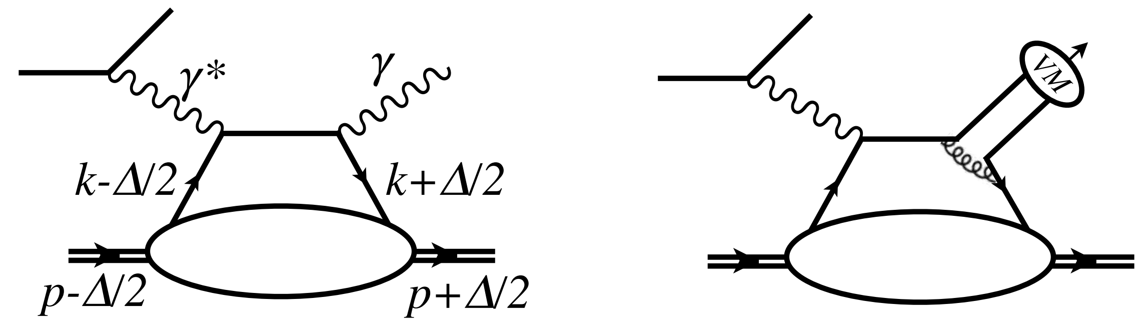

$$\gamma^*(q) + p(p) \rightarrow \gamma(q') + p(p')$$

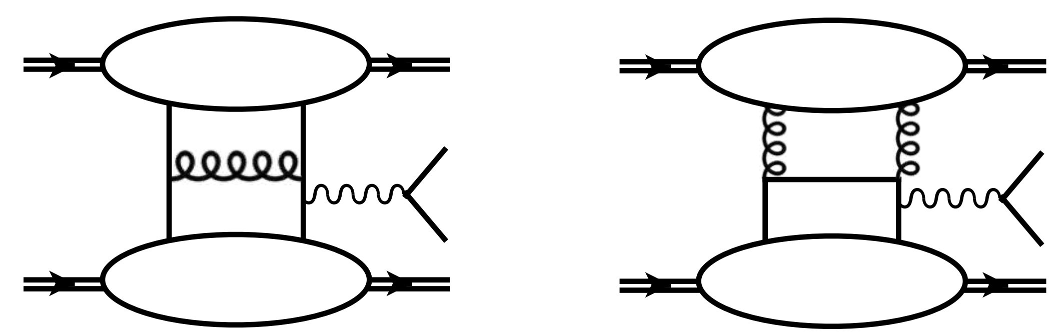

$$p(p_1) + p(p_2) \rightarrow p(p_1') + p(p_2') + \gamma(q')$$

Off-forward, skewed functions integrated over k_T

$\Delta = (p'-p)/2 \neq 0$

Off-diagonal matrix element of quark-quark operator

$$\langle p', \Lambda' | \bar{\psi}^q(-\frac{z}{2}) \Gamma \mathscr{W}(-\frac{z}{2}, \frac{z}{2}) \psi^q(\frac{z}{2}) | p, \Lambda \rangle$$

MC study: charmonia production

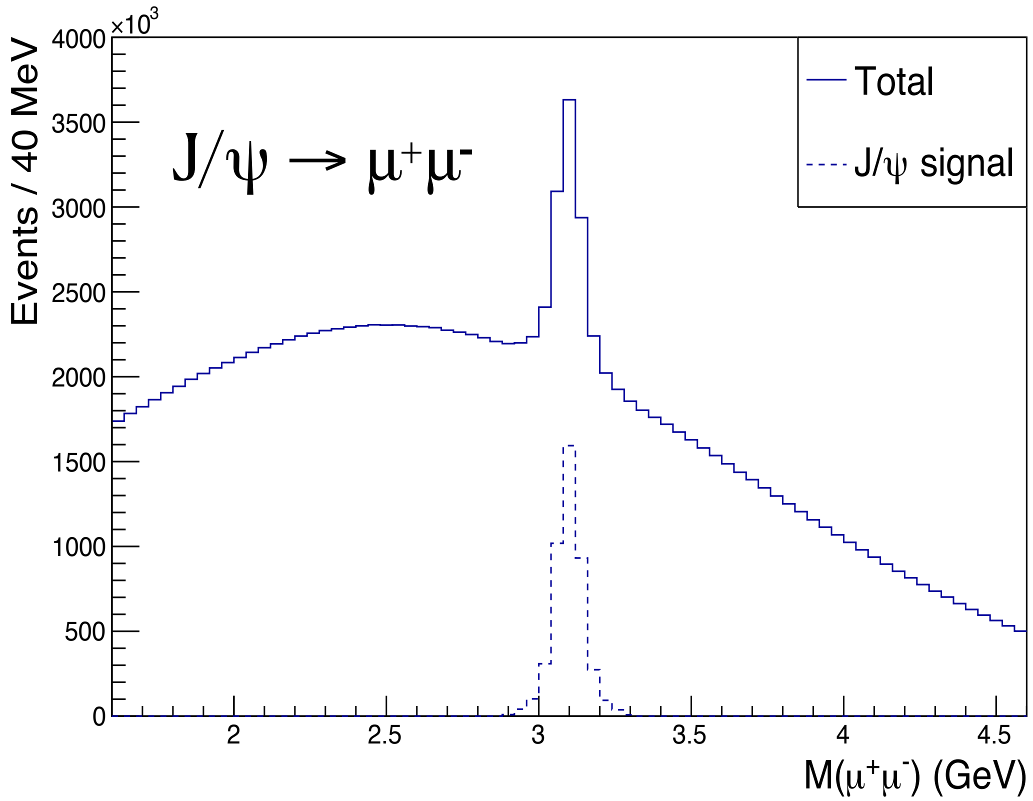

- 200 nb cross-section at $\sqrt{s}$=27 GeV, taking data for 10^7 s $\Rightarrow$ $12 \cdot 10^6$ decays $J/\psi \to \mu^+\mu^-$ in the detector
  - ~$4 \cdot 10^6$ events after all cuts
- TSSA probes the **Sivers function** in J/ψ production
- Two approaches describing hadronization stage
  - Non-Relativistic QCD factorization (NRQCD)
  - Improved Color-Evaporation Model (ICEM)
- GPM model prediction, A.Karpishkov, V.Saleev, M.Nefedov, arXiv:2008.07232

SIDIS1 GSF parametrization

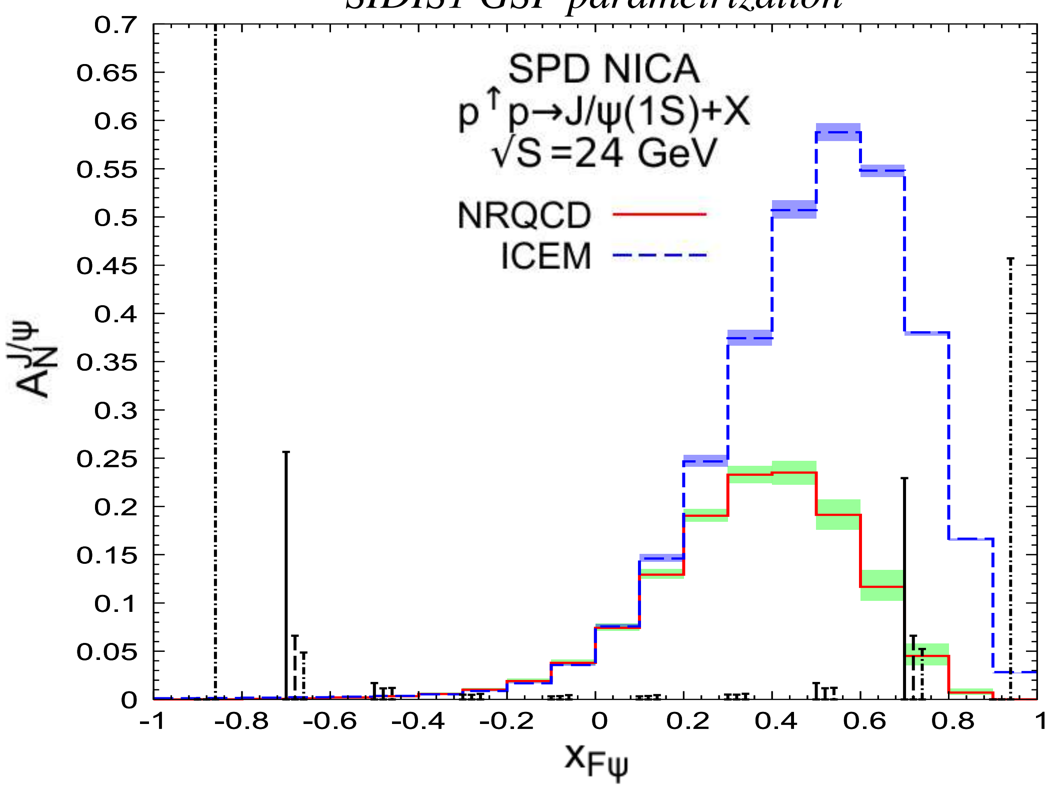

d'Alesio GSF parametrization

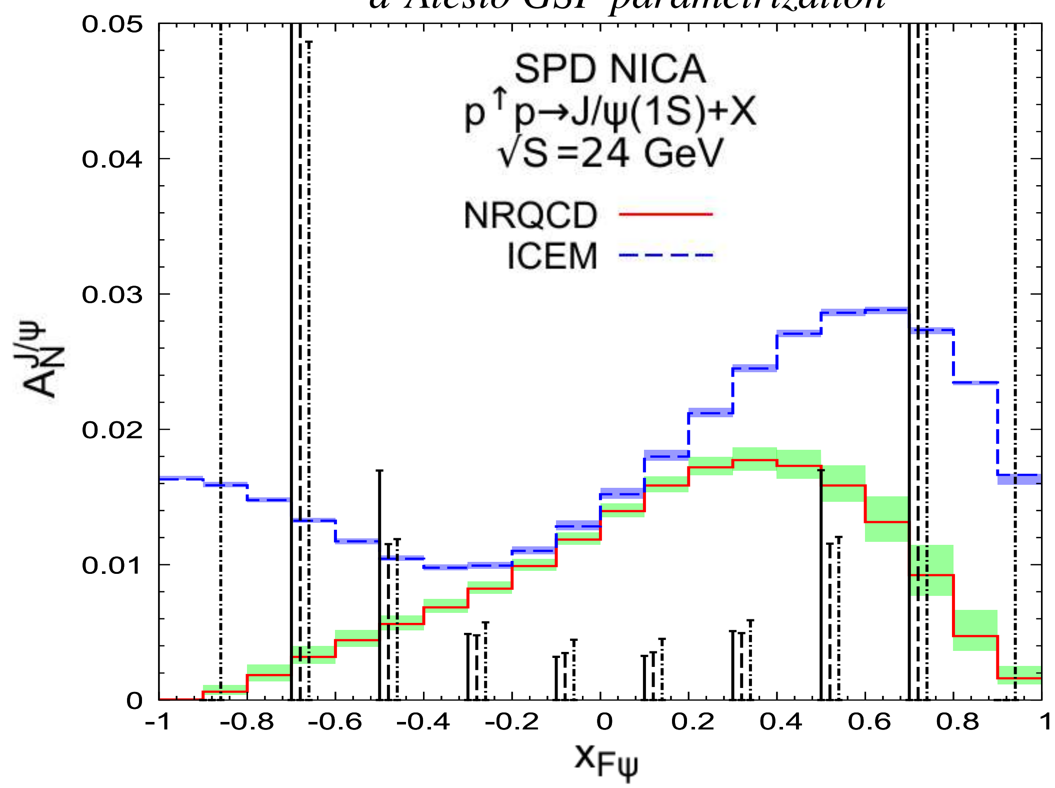

MC study: open charm production

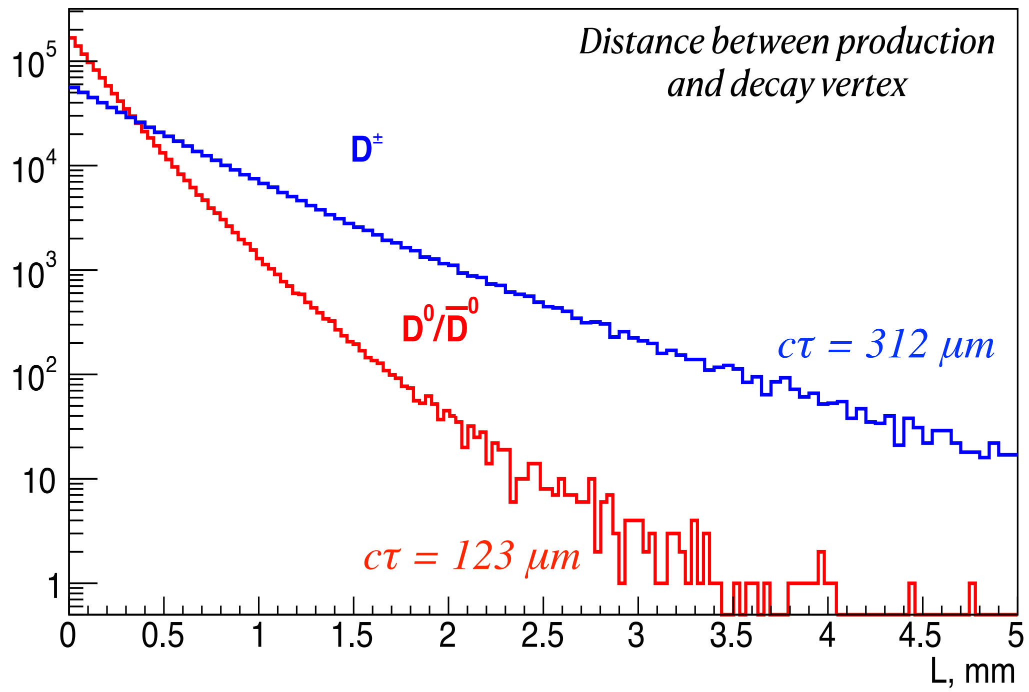

- "Golden" decay channels
  - $D^0 \rightarrow \pi^+ K^-$ and $D^+ \rightarrow \pi^+ K^- \pi^+$
- Typical momentum of D mesons is 2 GeV/c
- Selection criteria: χ^2, distance, angle
- Signal-to-background ratio for D^0
  - 1.3% for the DSSD-only option of VD
  - 3.9% for the DSSD+MAPS option of VD
- The expected Sivers contribution to SSA was estimated within GPM

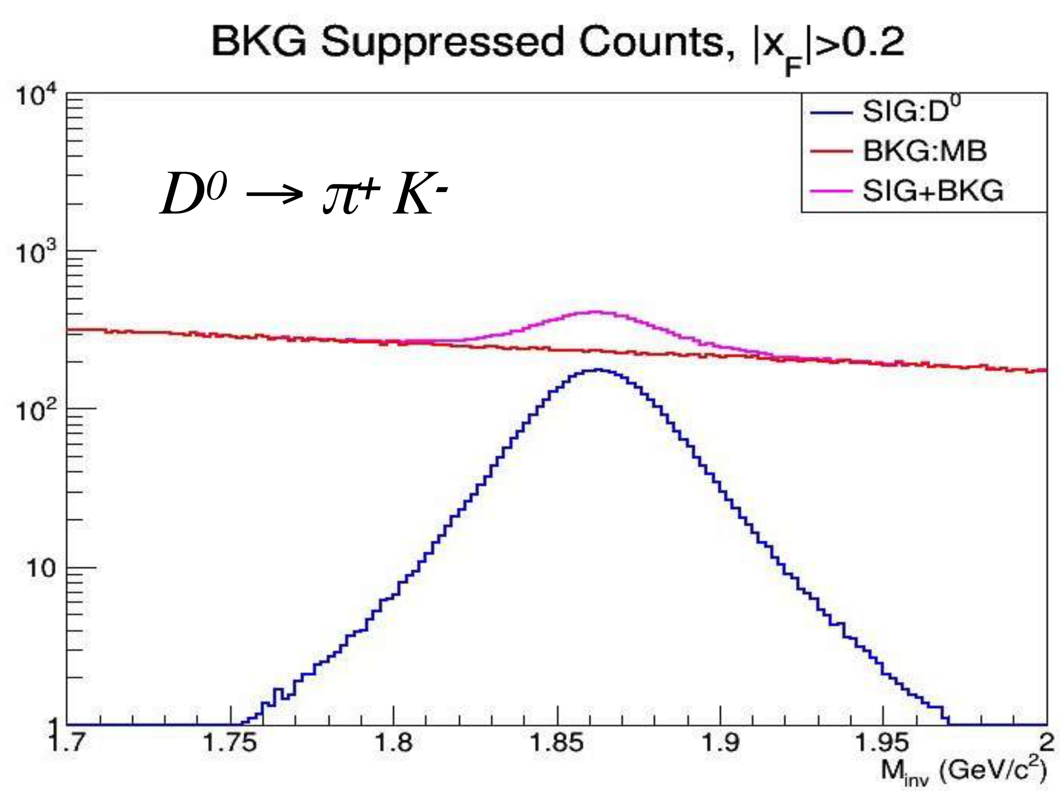

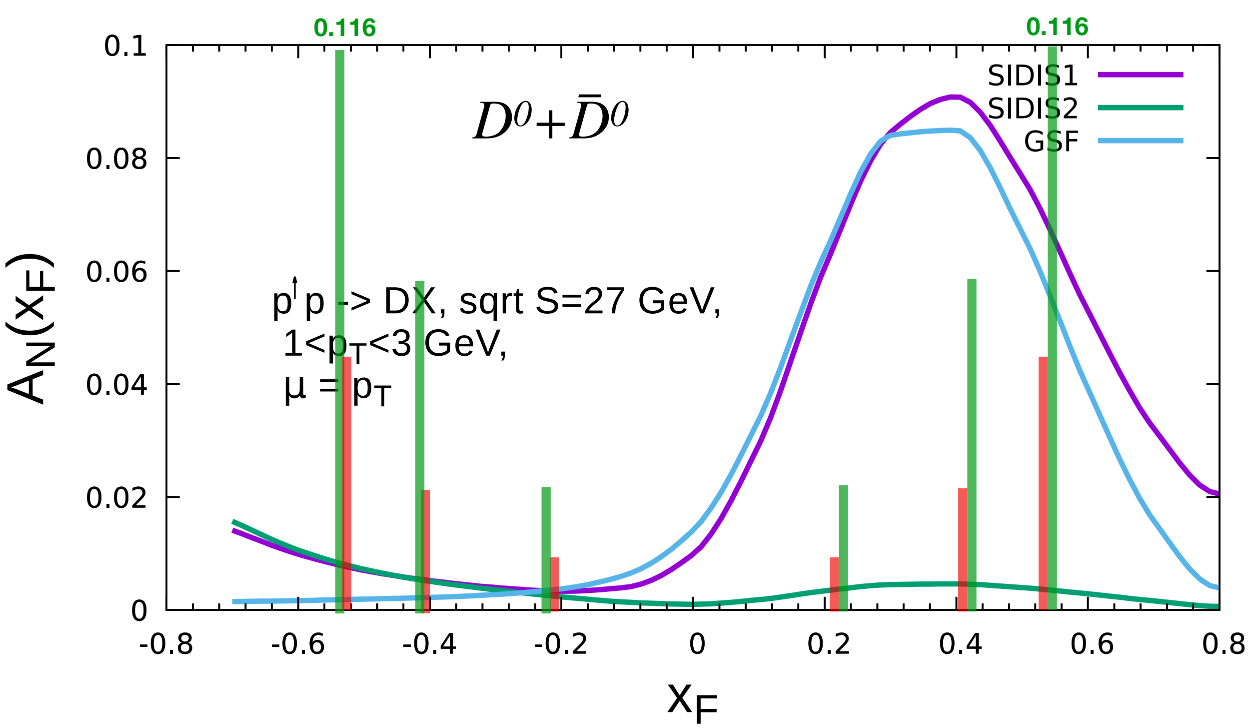

MC study: prompt photon production

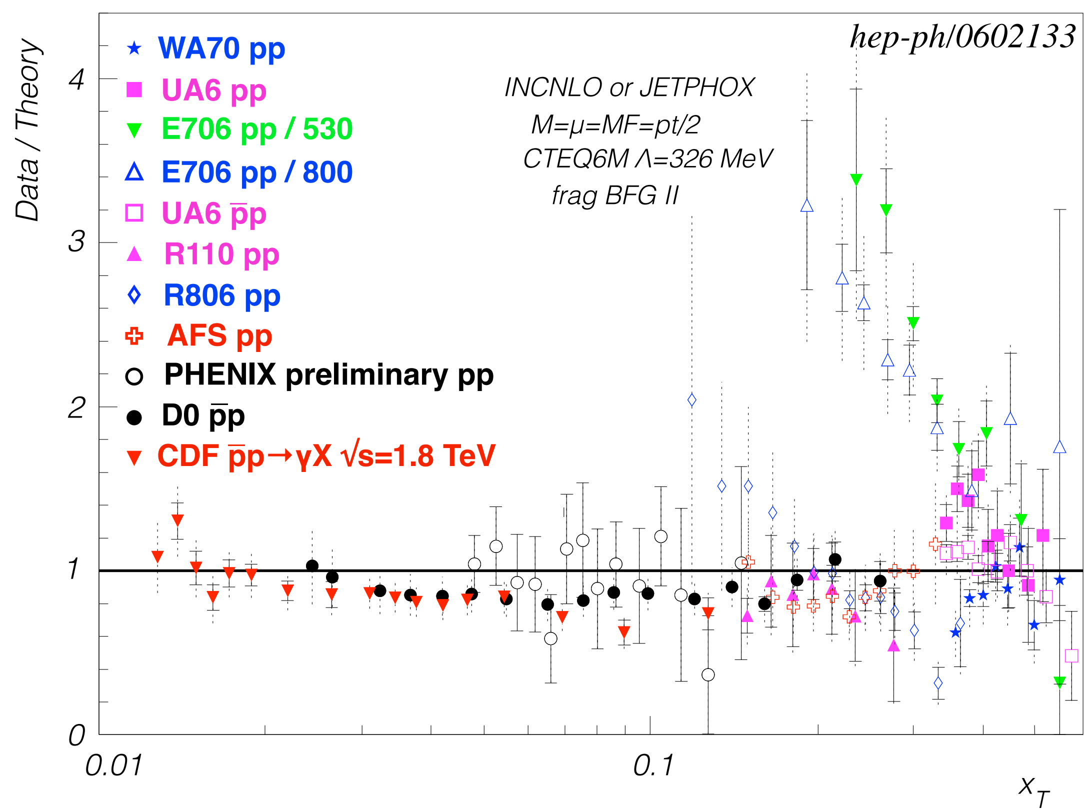

- Clean probe to study the Sivers DF and twist-3 correlation functions
- Proceeds without fragmentation ⇒ is exempt from the Collins effect
- Disagreement of theory and data at high x_T
- Main source of background: photons from decays of secondary π^0 and η. The rest of the decays contributes on the level of 3%
- Quark and gluon SF contributions were estimated separately within GPM